Supporting Information

for

Versatile coordination and C–H activation of a multi-donor phosphinoferrocene carboxamide ligand in Pd(II) complexes

Filip Horký, Karel Škoch, Ivana Císařová and Petr Štěpnička*

Department of Inorganic Chemistry, Faculty of Science, Charles University, Hlavova 2030, 128 40 Prague 2, Czech Republic

Contents

ALTERNATIVE SYNTHETIC ROUTES TOWARDS AMIDE 1

The original synthesis[S1] of amide **1** was based on the reaction between ferrocenecarbonyl chloride and 2-(diphenylphosphino)ethylamine in the presence of triethylamine. We have found that the acyl chloride can be replaced by other active acyl derivatives such as (1*H*-benzotriazol-1-ylcarbonyl)ferrocene (**S1** in method B, see Scheme S1) or pentafluorophenyl ferrocenecarboxylate (**S2** in method C). While the amidation reaction with **S1** proceeded very well (isolated yield: 87%), the coupling involving ester **S2** and 4-(dimethylamino)pyridine as the base catalyst did not reach completion during 20 h of reaction time and some of the starting material was recovered unchanged. Gratifyingly, the direct amide coupling (method A in Scheme S1) between ferrocenecarboxylic acid and 2-(diphenylphosphino)ethylamine in the presence of 1-ethyl-3-[3-(dimethylamino)propyl]carbodiimide (EDC) and 1-hydroxybenzotriazole (HOBt), produced pure amide **1** in a 83% yield after chromatography. Apparently, this method is the most practical, affording the target compound in a good yield and in pure form from readily available starting materials and in a single reaction step followed by simple purification.

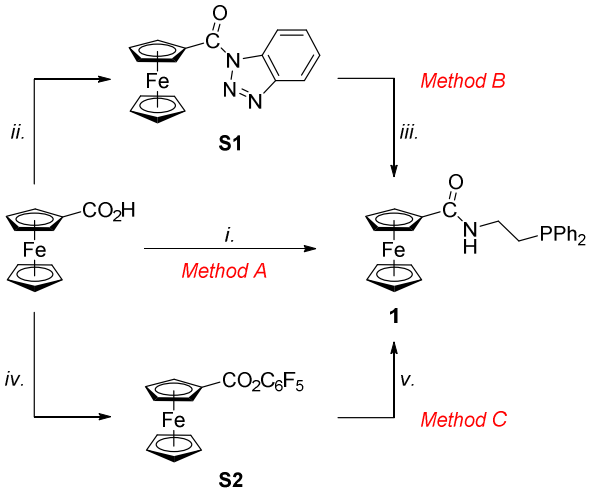

Scheme S1. Alternative syntheses of amide **1**.

Experimental details

Synthesis of (1H-Benzotriazol-1-ylcarbonyl)ferrocene (S1). Compound **S1** was prepared by following a previously reported general procedure.[S2, S3] Thus, ferrocenecarboxylic acid[S4] (460 mg, 2.0 mmol) and 1-(methylsulfonyl)-1*H*-benzotriazole[S2] (394 mg, 2.0 mmol) were dissolved in a mixture of dry THF (20 mL) and triethylamine (0.42 mL, 3.0 mmol), and the resulting mixture was heated at reflux under argon overnight. The volatiles were removed under vacuum, and the crude product was dissolved in chloroform (35 mL). The solution was washed with water (3× 10 mL), dried over anhydrous $MgSO_4$, and evaporated again. The crude product was purified by chromatography over silica gel using dichloromethane as the eluent. Subsequent evaporation afforded **2** as a deep red solid (662 mg, 76%).

^{1}H NMR ($CDCl_3$): δ 4.23 (s, 5 H, C_5H_5), 4.72 (vt, *J*′ = 2.2 Hz, 2 H, C_5H_4), 5.54 (vt, *J*′ = 2.2 Hz, 2 H, C_5H_4), 7.50-7.54 (m, 1 H, C_6H_4), 7.64-7.69 (m, 1 H, C_6H_4), 8.15 (dt, *J* = 8.3, 1.0 Hz, 1 H, C_6H_4), 8.38 (dt, *J* = 8.3, 1.0 Hz, 1 H, C_6H_4). ^{13}C{^{1}H} NMR ($CDCl_3$): δ 70.51 (s, C_5H_5), 70.99 (s, C^{ipso} of C_5H_4), 73.11 (s, CH of C_5H_4), 73.44 (s, CH of C_5H_4), 114.96 (s, CH of C_6H_4), 119.96 (s, CH of C_6H_4), 125.92 (s, CH of C_6H_4), 130.04 (s, CH of C_6H_4), 132.16 (s, C^{ipso} of C_6H_4), 145.45 (s, C^{ipso} of C_6H_4), 170.40 (s, C=O). The data match the reported ones.[S5]

{[[2-(Diphenylphosphino)ethyl]amino]carbonyl}ferrocene (1). Method A. Ferrocene-carboxylic acid (920 mg, 4.0 mmol) and 1-hydroxybenzotriazole (567 mg, 4.2 mmol) were mixed in dry dichloromethane (35 mL) and *N*,*N*-dimethylformamide (15 mL). The resulting suspension was cooled in an ice bath and treated with neat 1-ethyl-3-[3-(dimethylamino)-propyl]carbo-diimide (0.74 ml, 4.2 mmol) with continuous stirring. After the mixture was stirred for 30 min, 2-(diphenylphosphino)ethylamine (1.00 g, 4.4 mmol) was added and the stirring was continued at 0 °C for 30 min and at room temperature for another 12 h. Then, the reaction mixture was washed with saturated aqueous $NaHCO_3$ and brine, dried over anhydrous $MgSO_4$, and evaporated under vacuum, leaving a rusty brown crude product. Purification by column chromatography (silica gel, dichloromethane-methanol 20:1) followed by evaporation afforded pure amide **1** as a rusty orange solid (1.47 g, 83%). The second band contained a small amount of the corresponding phosphine oxide **2** (ca. 100 mg, 5%).

Method B. A solution of compound **S1** (237 mg, 0.72 mmol) in THF (15 mL) was slowly introduced to 2-(diphenylphosphino)ethylamine (181 mg, 0.79 mmol) dissolved in the same solvent (4 mL) while stirring and cooling in an ice bath. After the addition was complete (15 min), the stirring was continued at 0 °C for 30 min and then at room temperature for 12 h. Next, the reaction mixture was evaporated and the solid residue was purified by column chromatography as described above to give analytically pure **1**. Yield: 274 mg (87%).

Method C. A reaction flask was charged with ester **S2**[S6] (594 mg, 1.5 mmol), flushed with argon and sealed with a rubber septum. Dry dichloromethane was introduced (20 mL), immediately followed by 4-(dimethylamino)pyridine (49 mg, 0.40 mmol in 2 mL of CH_2Cl_2) and neat 2-(diphenylphosphino)ethylamine (13 mg, 1.8 mmol). The resulting mixture was stirred at room temperature for 20 h and evaporated under vacuum, leaving crude product, which was purified by column chromatography as described above. Evaporation of the first red band recovered unreacted ester **S2** (168 mg, 28%), and the second orange band provided amide **1** (452 mg, 68%).

Analytical data for **1**. ^{1}H NMR ($CDCl_3$): δ 2.40 (t, $^3J_{HH}$ = 7.1 Hz, 2 H, PCH_2), 3.54 (m, 2 H, $NHCH_2$), 4.19 (s, 5 H, C_5H_5), 4.31 (vt, J' = 1.9 Hz, 2 H, C_5H_4), 4.57 (vt, J' = 2.0 Hz, 2 H, C_5H_4), 5.92 (t, $^3J_{HH}$ = 4.9 Hz, 1 H, NH), 7.31-7.39 (m, 6 H, PPh_2), 7.44-7.50 (m, 4 H, PPh_2). ^{13}C{^{1}H} NMR ($CDCl_3$): δ 28.79 (d, $^1J_{PC}$ = 13 Hz, PCH_2), 36.87 (d, $^2J_{PC}$ = 19 Hz, $NHCH_2$), 68.04 (s, CH C_5H_4), 69.74 (s, C_5H_5), 70.33 (s, CH C_5H_4), 76.03 (s, C^{ipso} C_5H_4), 128.64 (d, $^3J_{PC}$ = 7 Hz, CH^{meta} PPh_2), 128.87 (s, CH^{para} PPh_2), 132.74 (d, $^2J_{PC}$ = 19 Hz, CH^{ortho} PPh_2), 137.64 (d, $^1J_{PC}$ = 12 Hz, C^{ipso} PPh_2), 170.18 (s, C=O). ^{31}P{^{1}H} NMR ($CDCl_3$): δ −20.8 (s). The NMR data matched those in the literature.[1] IR (Nujol): ν_{max} 3273 br m, 3079 w, 1623 s, 1544 s, 1435 m, 1298 m, 1223 w, 1178 m, 1108 w, 1023 m, 998 n, 825 m, 748 m, 733 s, 700 s, 537 w, 510 m, 484 m, 465 m, 439 m cm^{-1}.

Synthesis of phosphine oxide 1O. Amide **1** (88 mg, 0.2 mmol) was dissolved in reagent-grade acetone (5 mL) and the solution was cooled on ice. Aqueous hydrogen peroxide (0.1 mL 30%, ca. 1 mmol) was added drop-wise and the reaction mixture was stirred for 10 min. Next, saturated aqueous $Na_2S_2O_3$ (5 mL) was added and the mixture was stirred for another 30 min to destroy the excess of H_2O_2. The acetone was removed under vacuum and the organic residue was extracted with dichloromethane. The combined organic layers were dried over $MgSO_4$ and evaporated, leaving pure phosphine oxide **1O** as an orange solid (80 mg, 87%). Crystals of hemihydrate, suitable for X-ray diffraction analysis, were grown from ethyl acetate-hexane.

^{1}H NMR ($CDCl_3$): δ 2.57 (dt, J = 10.1, 6.4 Hz, 2 H, PCH_2), 3.75 (dq, J = 18.6, 5.6 Hz, 2 H, $NHCH_2$), 4.19 (s, 5 H, C_5H_5), 4.31 (vt, J' = 2.0 Hz, 2 H, C_5H_4), 4.70 (vt, J' = 2.0 Hz, 2 H, C_5H_4), 7.37 (br t, 1 H, NH), 7.47-7.56 (m, 6 H, PPh_2), 7.75-7.80 (m, 4 H, PPh_2). ^{13}C{^{1}H} NMR ($CDCl_3$): δ 28.98 (d, $^1J_{PC}$ = 71 Hz, PCH_2), 33.94 (d, $^2J_{PC}$ = 5 Hz, $NHCH_2$), 68.27 (s, CH C_5H_4), 69.74 (s, C_5H_5), 70.36 (s, CH C_5H_4), 75.81 (s, C^{ipso} C_5H_4), 128.93 (d, J_{PC} = 12 Hz, CH^{meta} PPh_2), 130.61 (d, $^2J_{PC}$ = 10 Hz, CH^{ortho} PPh_2), 132.16 (d, $^4J_{PC}$ = 3 Hz, CH^{para} PPh_2), 132.23 (d, $^1J_{PC}$ = 100 Hz, C^{ipso} PPh_2), 170.64 (s, C=O). ^{31}P{^{1}H} NMR ($CDCl_3$): δ 34.7 (s). ESI+ MS: *m/z* 458 ($[M + H]^+$), 480 ($[M + Na]^+$), 496 ($[M + K]^+$). IR (Nujol): ν_{max} 3284 br m, 3087 w, 3058 w, 1646 s, 1559 s, 1299 s, 1217 w, 1181 s, 1173 s, 1121 m, 1103 m, 997 w, 970 w, 909 w, 877 w, 851 w, 839 w, 807 m, 755 m, 750 m, 729 s, 719 m, 699 s, 693 m, 592 w, 559 w, 519 s, 502 w, 485 w, 467 w cm^{-1}. Anal. Calc. for $C_{25}H_{24}FeNO_2P{\cdot}0.5H_2O$ (466.3): C 64.39, H 5.40, N 3.00%. Found: C 64.39, H 5.32, N 2.75% (crystallised sample).

Synthesis of phosphine selenide 1Se. Phosphine **1** (53.0 mg, 0.12 mmol) and NaSeCN (21.7 mg, 0.15 mmol) were reacted in a mixture of dichloromethane and methanol (10 mL each) at room temperature overnight. Following evaporation under vacuum, the crude product was dissolved in dichloromethane (10 mL). The solution was filtered through a PTFE syringe filter (0.45 μm pore size) and precipitated by adding pentane. The separated solid was filtered off and dried under vacuum. Yield of **1Se**: orange solid (30 mg, 47%)

^{1}H NMR ($CDCl_3$): δ 2.95-3.01 (m, 2 H, PCH_2), 3.74-3.83 (m, 2 H, NHCH_2), 4.18 (s, 5 H, C_5H_5), 4.30 (vt, J' = 2.0 Hz, 2 H, C_5H_4), 4.61 (vt, J' = 2.0 Hz, 2 H, C_5H_4), 6.96 (t, J = 5.7 Hz, 1 H, NH), 7.43-7.53 (m, 6 H, PPh_2), 7.83-7.90 (m, 4 H, PPh_2). ^{13}C {^{1}H} NMR ($CDCl_3$): δ 31.89 (d, J_{PC} = 50 Hz, PCH_2), 34.84 (d, J_{PC} = 2 Hz, $NHCH_2$), 68.19 (s, C_5H_4), 69.74 (s, C_5H_5), 70.40 (s, C_5H_4), 75.52 (s, C_{ipso} of C_5H_4) 128.87 (d, J_{PC} = 12 Hz, CH of PPh_2), 130.91 (d, J_{PC} = 73 Hz, C_{ipso} of PPh_2), 131.49 (d, J_{PC} = 10 Hz, CH of PPh_2), 131.84 (d, J_{PC} = 3 Hz, CH of PPh_2), 170.60 (s, CO). ^{31}P{^{1}H} NMR ($CDCl_3$): δ 30.5 (s with ^{77}Se satellites, $^{1}J_{SeP}$ = 714 Hz). IR (Nujol):ν_{max} 3257 br s, 3090 m, 1622 s, 1549 s, 1458, 1436 s, 1411 w, 1379 m, 1305 m, 1225 w, 1178 m, 1106 m, 1096 m, 1019 m, 998 m, 904 w, 835 w, 813 m, 745 s, 693 m, 530 s, 515 m, 499 m, 466 m cm^{-1}. ESI + MS: *m/z* 521 (M^+), 544 ([M + Na]$^+$). Anal. Calc. for $C_{25}H_{24}ONFeP{\cdot}0.1CH_2Cl_2$ (532.7): C 56.94, H 4.59, N 2.66%. Found: C 56.81, H 4.73, 2.56%.

X-RAY CRYSTALLOGRAPHY

Table S1. Summary of relevant crystallographic data and refinement parameters

Compound	**1O**·½H_2O	*trans*-**2a**·MeCN	*trans*-**2b**·3$C_2H_4Cl_2$	*trans*-**2c**·2.5$C_2H_4Cl_2$
Formula	$C_{25}H_{25}FeNO_{2.5}P$	$C_{52}H_{51}Cl_2Fe_2N_3O_2P_2Pd$	$C_{56}H_{60}Br_2Cl_6Fe_2N_2O_2P_2Pd$	$C_{55}H_{58}Cl_5Fe_2I_2N_2O_2P_2Pd$
M	466.28	1100.90	1445.62	1490.12
Crystal system	triclinic	monoclinic	tetragonal	triclinic
Space group	$P\bar{1}$ (no. 2)	$P2_1/c$ (no. 14)	$I4_1/a$ (no. 88)	$P\bar{1}$ (no. 2)
T/K	150(2)	150(2)	150(2)	150(2)
a/Å	8.5987(3)	22.3817(5)	24.6811(7)	9.9817(3)
b/Å	11.4331(4)	9.5691(2)	24.6811(7)	12.5696(3)
c/Å	12.2092(5)	22.7215(5)	19.4321(7)	24.8429(6)
α/°	80.142(1)	90	90	104.189(1)
β/°	71.848(1)	94.325(1)	90	91.525(1)
γ/°	75.265(1)	90	90	106.340(1)
V/Å^3	1097.50(7)	4852.5(2)	11837.2(8)	2884.5(1)
Z	2	4	8	2
F(000)	486	2248	5808	1474
μ(Mo Kα)/mm^{-1}	0.784	1.176	2.502	2.204
Diffrns collected	19091	34160	20300	38087
Independent diffrns	5020	9533	5815	13212
Observed[a] diffrns	4355	7296	4132	11117
R_{int}[b]/%	2.51	4.75	6.39	2.40
No. of parameters	280	578	332	653
R[b] obsd diffrns/%	2.98	3.33	5.15	3.13
R, wR[b] all data/%	3.70, 7.59	5.26, 7.67	9.27, 14.13	4.07, 7.82
Δρ/e Å^{-3}	0.50, −0.37	0.48, −0.48	2.72, −0.75	1.75, −1.20

[a] Diffractions with $I > 2\sigma(I)$. [b] Definitions: $R_{int} = \Sigma \left| F_o^2 - F_o^2(\text{mean}) \right| / \Sigma F_o^2$, where F_o^2(mean) is the average intensity of symmetry-equivalent diffractions. $R = \Sigma \left| \left| F_o \right| - \left| F_c \right| \right| / \Sigma \left| F_o \right|$, $wR = [\Sigma\{w(F_o^2 - F_c^2)^2\}/\Sigma w(F_o^2)^2]^{1/2}$.

Table S1 continued

Compound	**4a**·CH_2Cl_2	**5**·3$CHCl_3$·Et_2O	**8**
Formula	$C_{53}H_{50}Cl_2F_6Fe_2I_2N_2O_8P_2PdS_2$	$C_{56}H_{58}Cl_6Fe_2N_2O_3P_2Pd$	$C_{34}H_{35}FeN_2OPPd$
M	1372.01	1299.78	680.86
Crystal system	monoclinic	monoclinic	triclinic
Space group	$P2_1$ (no. 4)	$C2/c$ (no. 15)	$P\bar{1}$ (no. 2)
T/K	150(2)	150(2)	150(2)
a/Å	13.3402(3)	33.6489(11)	10.9881(2)
b/Å	10.6845(2)	13.9071(4)	11.6075(2)
c/Å	19.5177(4)	25.6588(10)	12.5380(3)
α/°	90	90	112.701(1)
β/°	97.843(1)	115.785(2)	95.227(1)
γ/°	90	90	97.821(1)
V/Å^3	2755.9(1)	10811.7(7)	1443.39(5)
Z	2	8	2
F(000)	1388	5296	696
μ(Mo Kα)/mm^{-1}	1.149	1.261	1.212
Diffrns collected	23388	75271	18414
Independent diffrns	10199	12403	6610
Observed[a] diffrns	9369	10430	6246
R_{int}[b]/%	2.97	2.77	1.58
No. of parameters	704	568	387
R[b] obsd diffrns/%	3.26	3.71	2.01
R, wR[b] all data/%	3.87, 7.43	4.73, 10.0	2.19, 4.87
Δρ/e Å^{-3}	1.01, −0.94	1.33, −1.55	0.52, −0.36

Additional structural diagrams

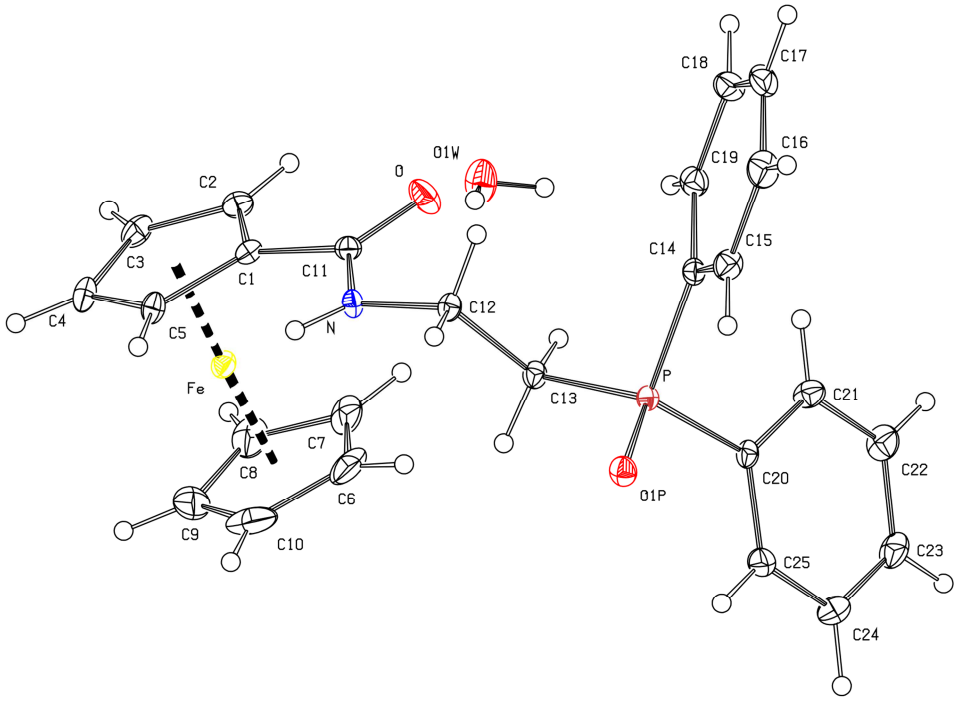

Figure S1. PLATON plot of the molecular structure of **1O**·½H_2O with displacement ellipsoids set to 30% probability.

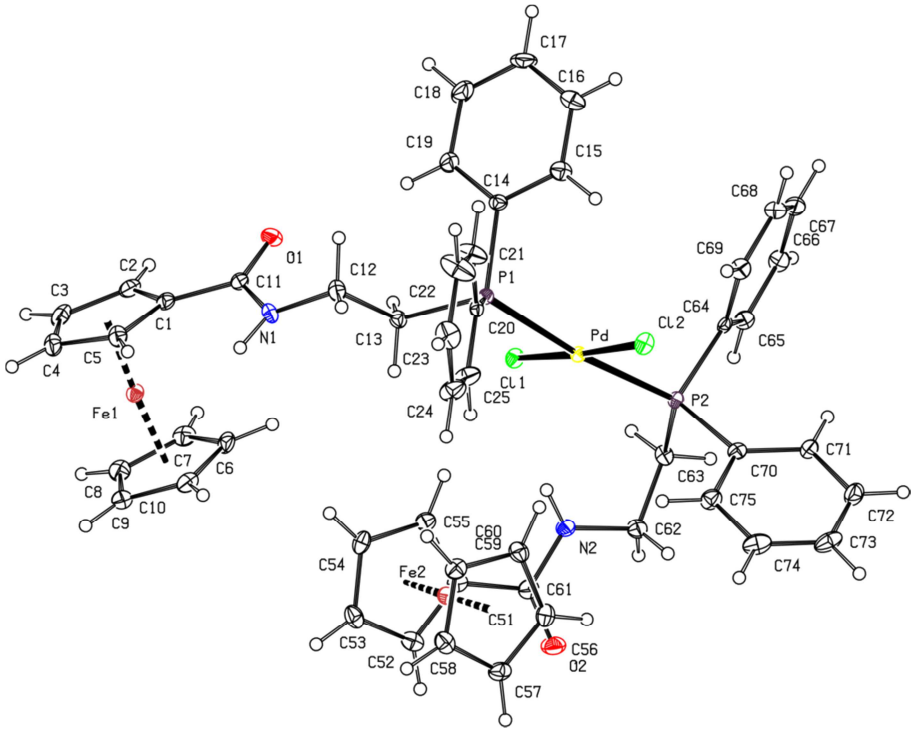

Figure S2. PLATON plot of the complex molecule in the structure of *trans*-**2a**·MeCN. Displacement ellipsoids enclose the 30% probability level.

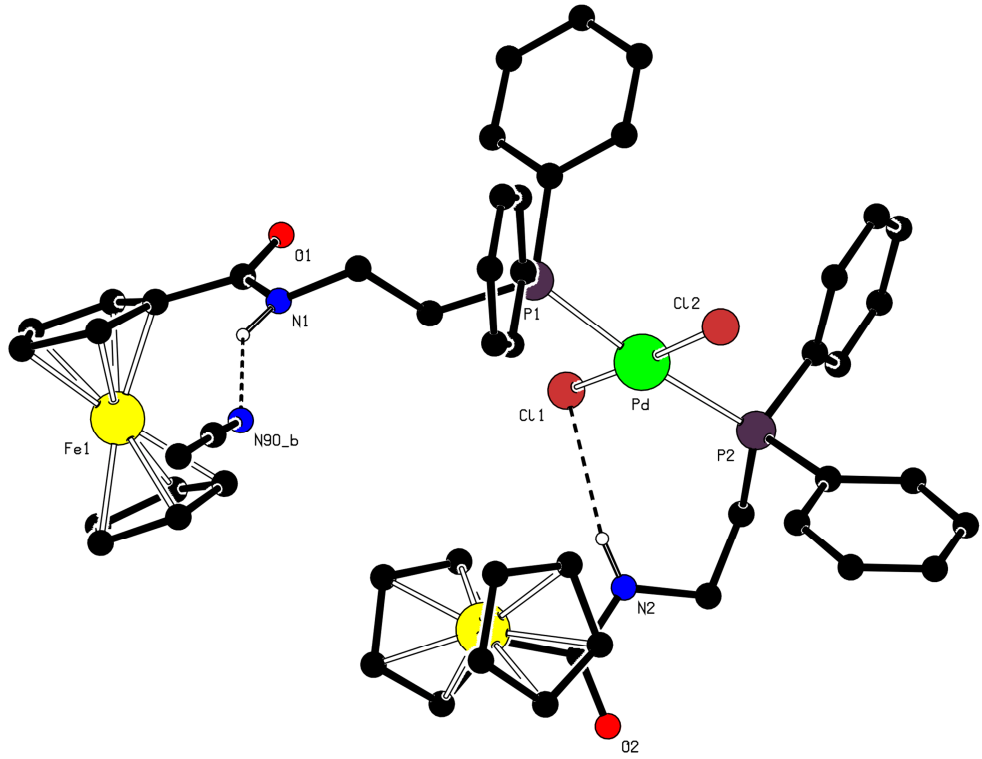

Figure S3. Hydrogen-bonding interaction in the structure of *trans*-**2a**·MeCN. For clarity, all hydrogen atoms except those in the NH groups were omitted.

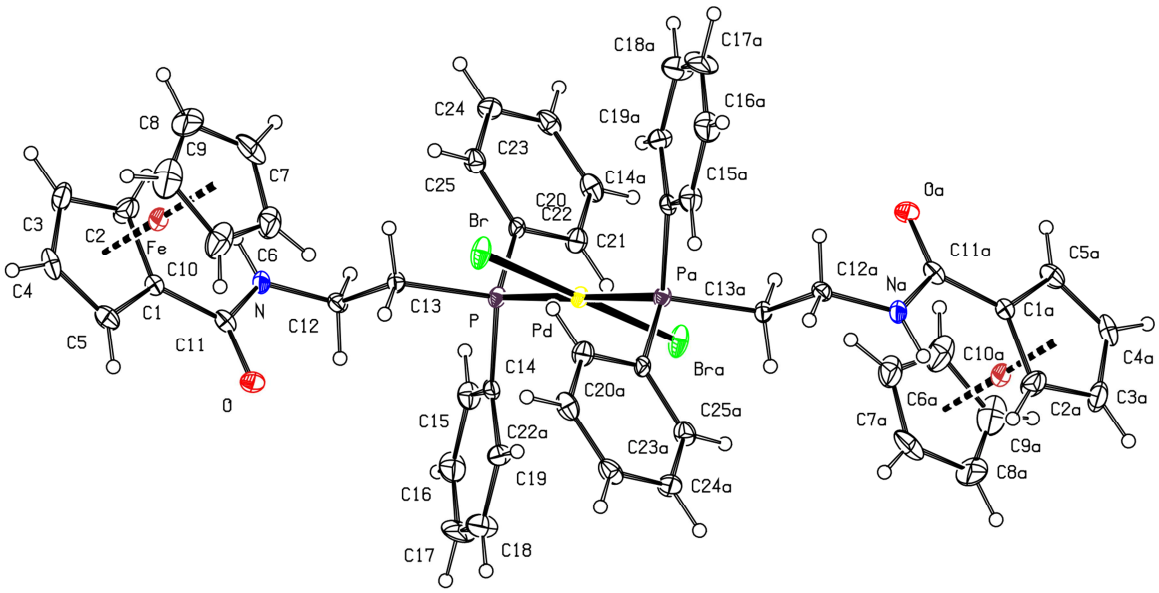

Figure S4. PLATON plot of the complex molecule in the structure of *trans*-**2b**·$3C_2H_4Cl_2$ showing displacement ellipsoids at the 30% probability level.

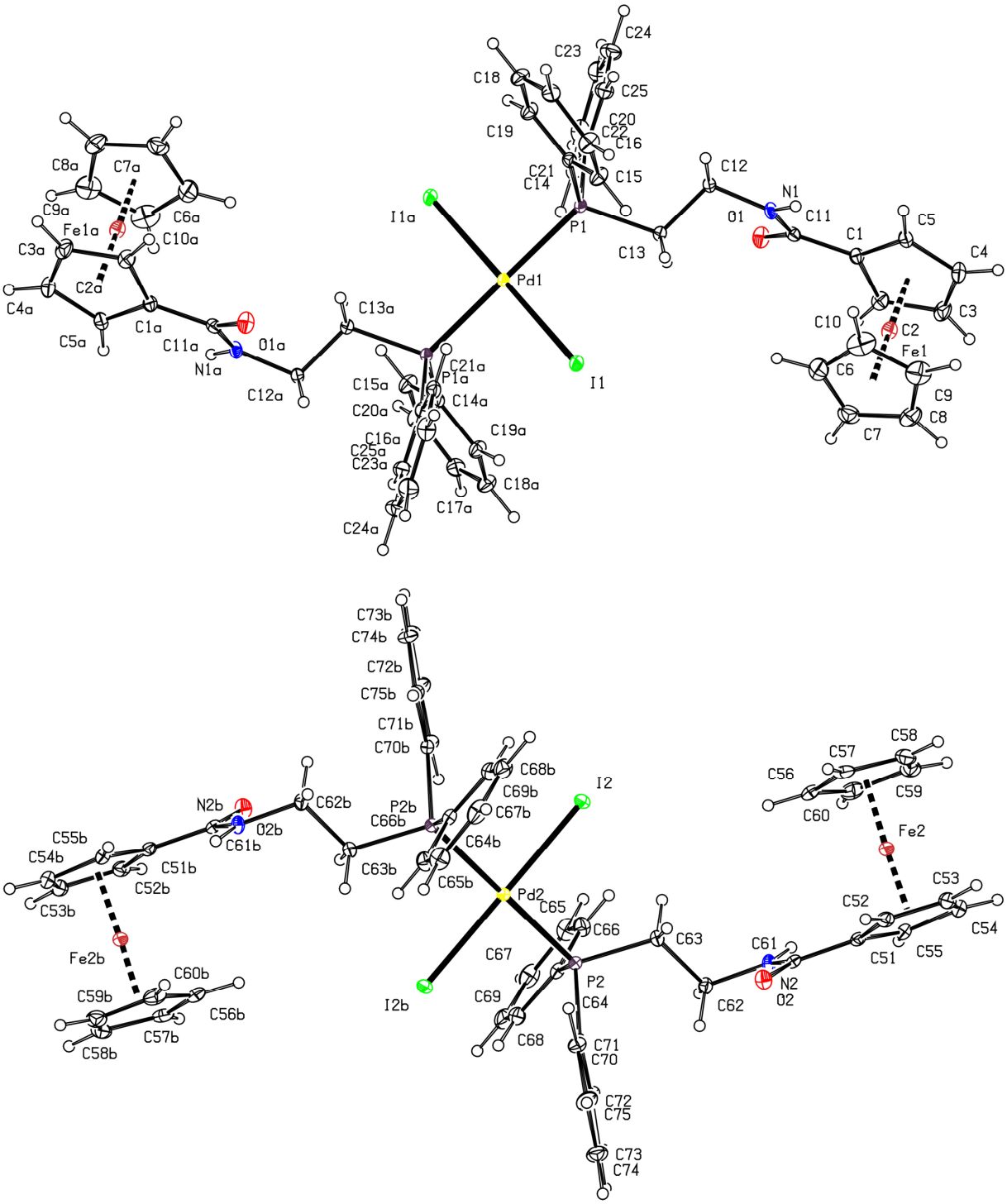

Figure S5. PLATON plots of the structurally independent complex molecules in the structure of *trans*-**2c**·2.5$C_2H_4Cl_2$ showing displacement ellipsoids at the 30% probability level.

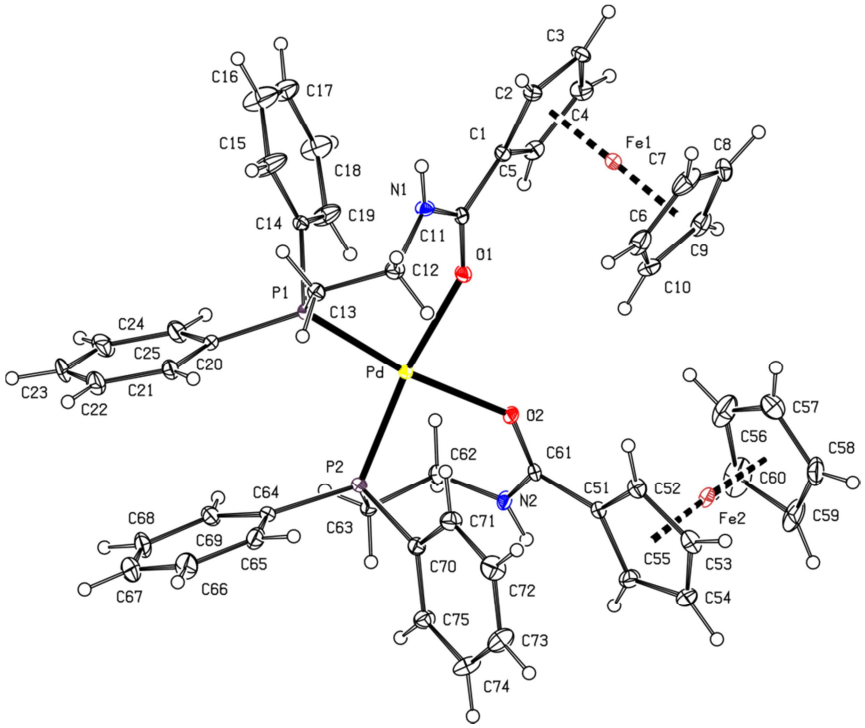

Figure S6. PLATON plot of the complex cation in the structure of **4a**·CH_2Cl_2 showing the displacement ellipsoids at the 30% probability level.

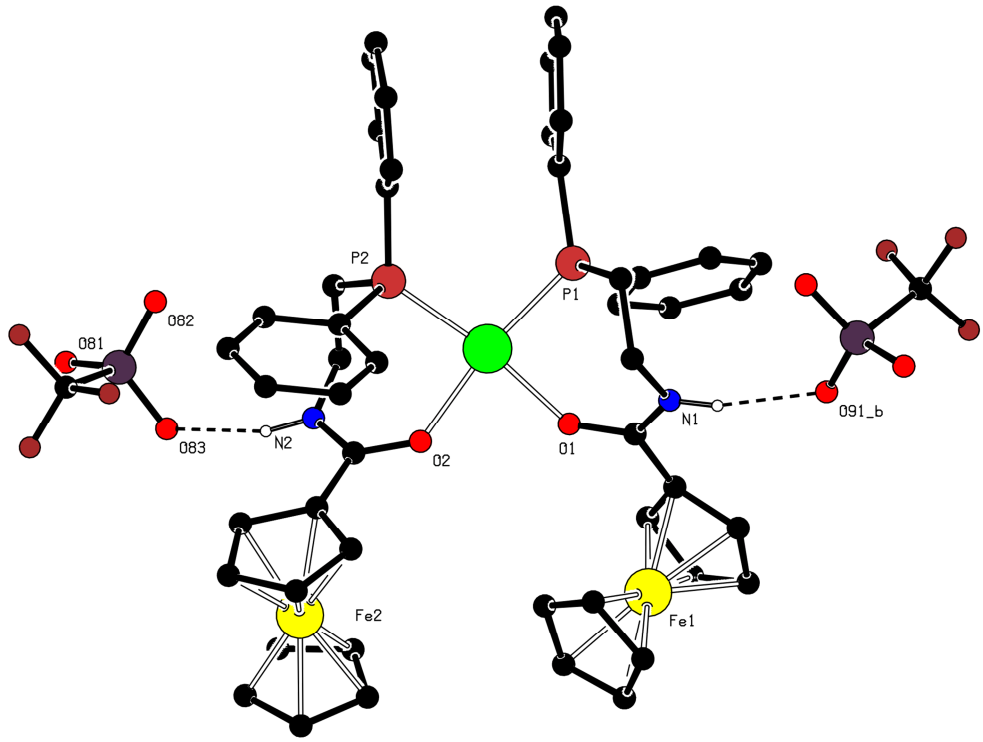

Figure S7. N-H···O hydrogen bonds in the structure of **4a**·CH_2Cl_2. The solvent molecule was omitted for clarity.

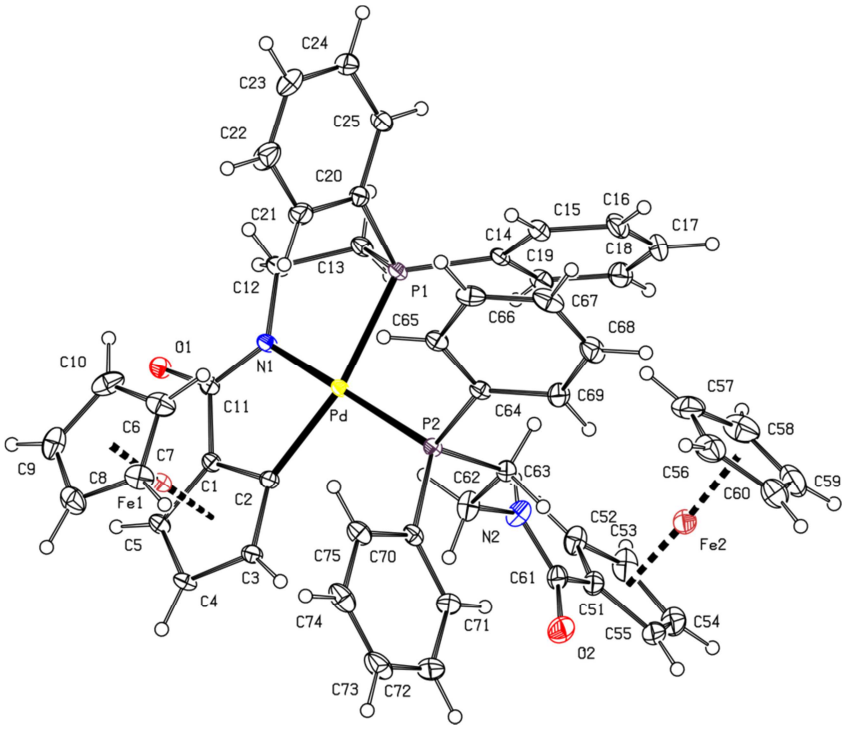

Figure S8. PLATON plot of the molecular structure of **5**·3$CHCl_3$·Et_2O with probability ellipsoids at the 30% probability level.

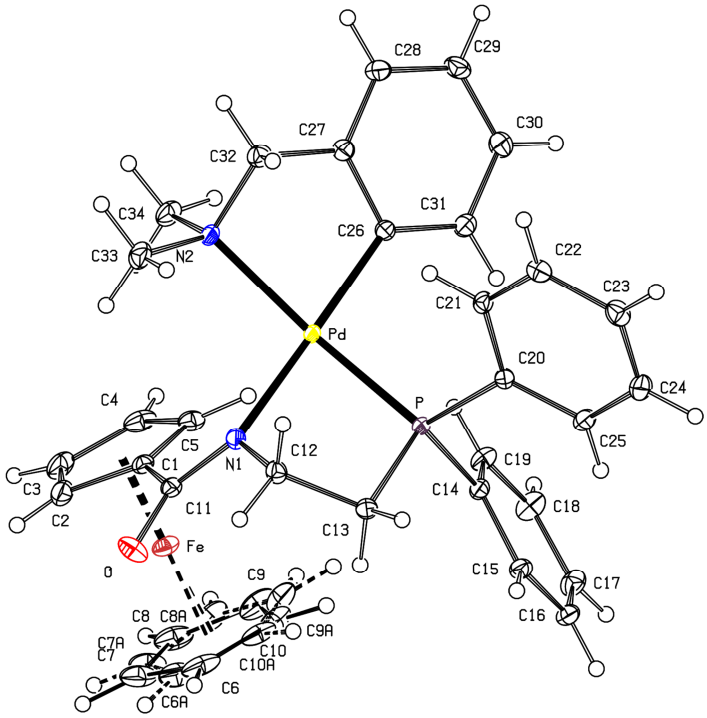

Figure S9. PLATON plot of the molecular structure of **8** showing probability ellipsoids at the 30% probability level and both orientations of the disordered cyclopentadienyl ring.

COPIES OF THE NMR SPECTRA

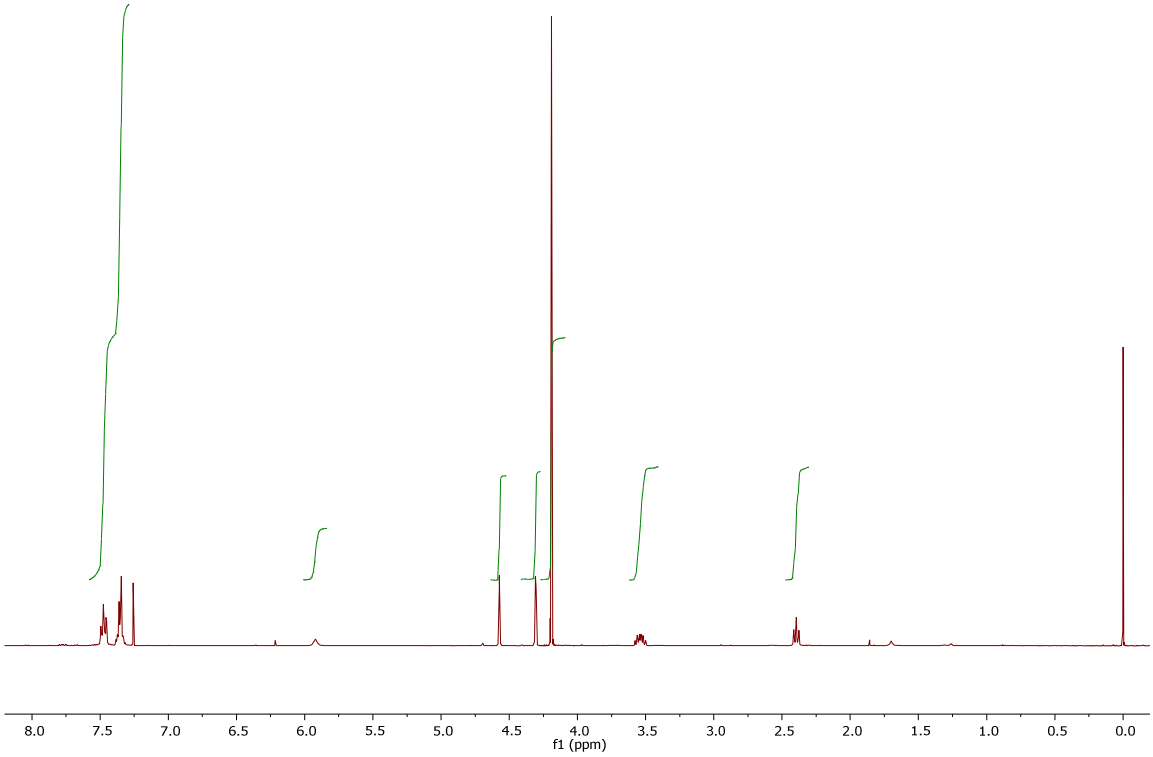

Figure S10. ^{1}H NMR (400 MHz, $CDCl_3$) spectrum of **1**.

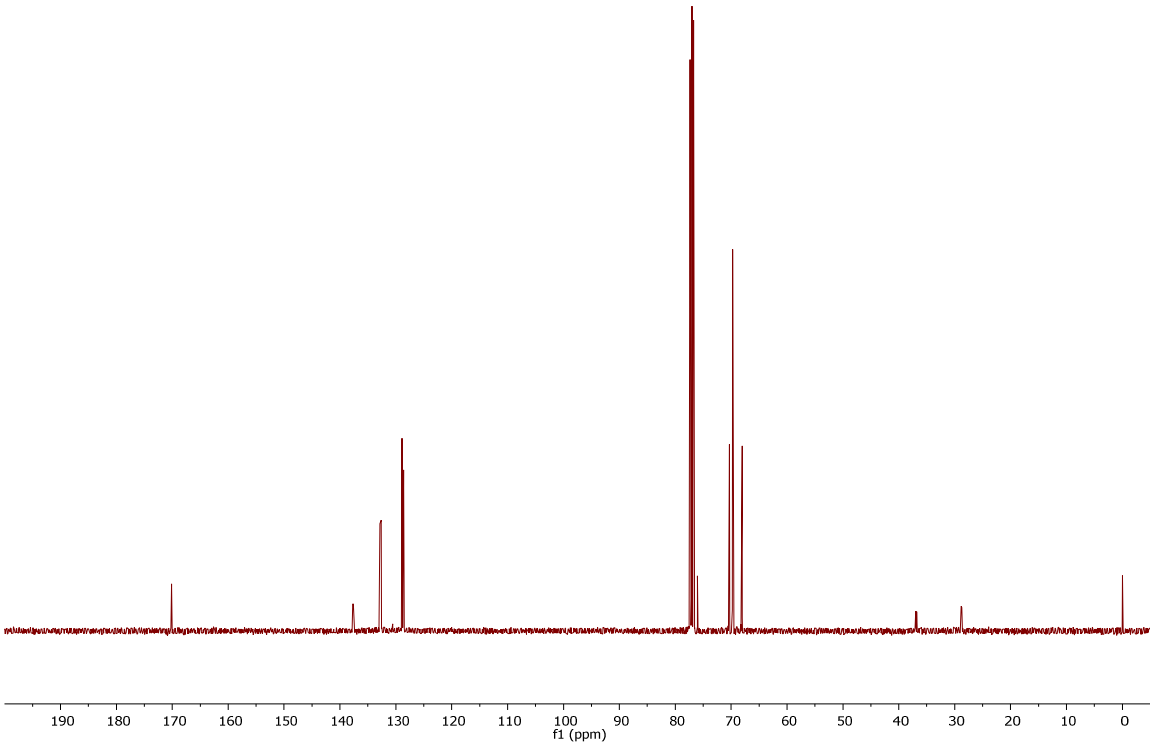

Figure S11. $^{13}C\{^{1}H\}$ NMR (101 MHz, $CDCl_3$) spectrum of **1**.

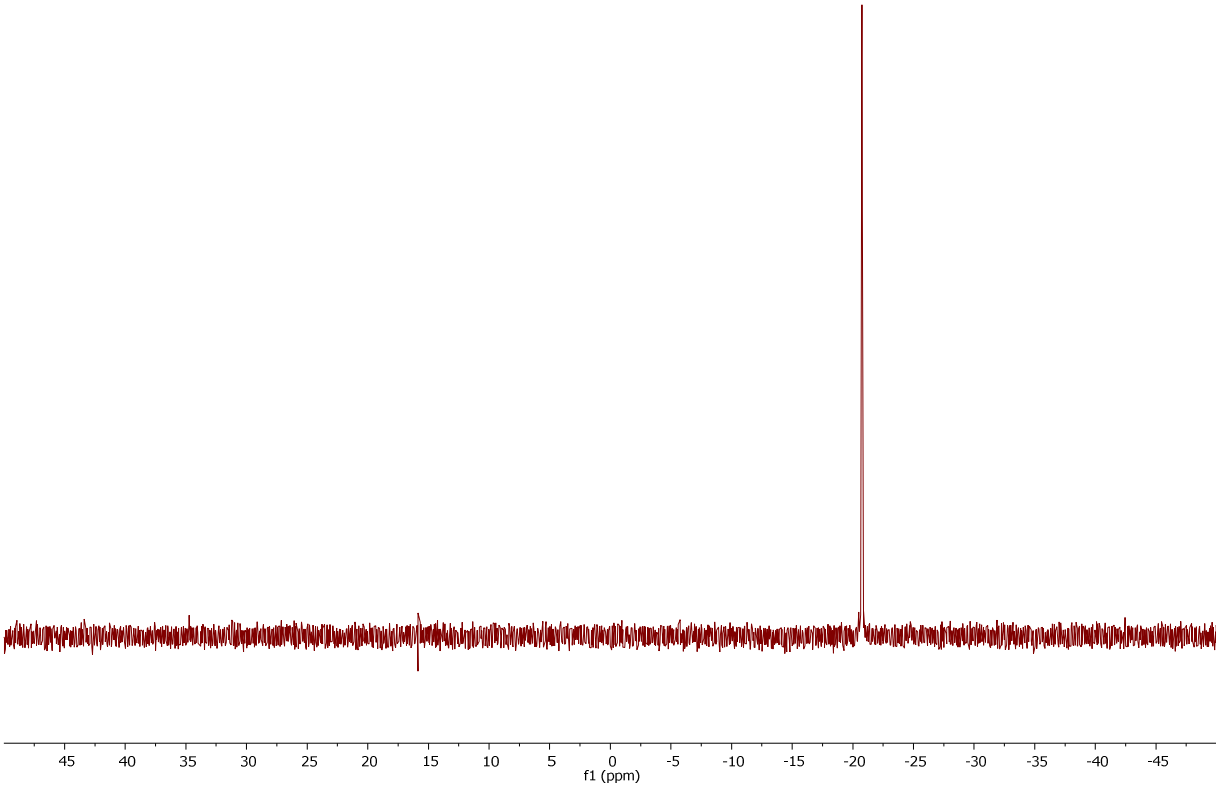

Figure S12. $^{31}P\{^{1}H\}$ NMR (162 MHz, $CDCl_3$) spectrum of **1**.

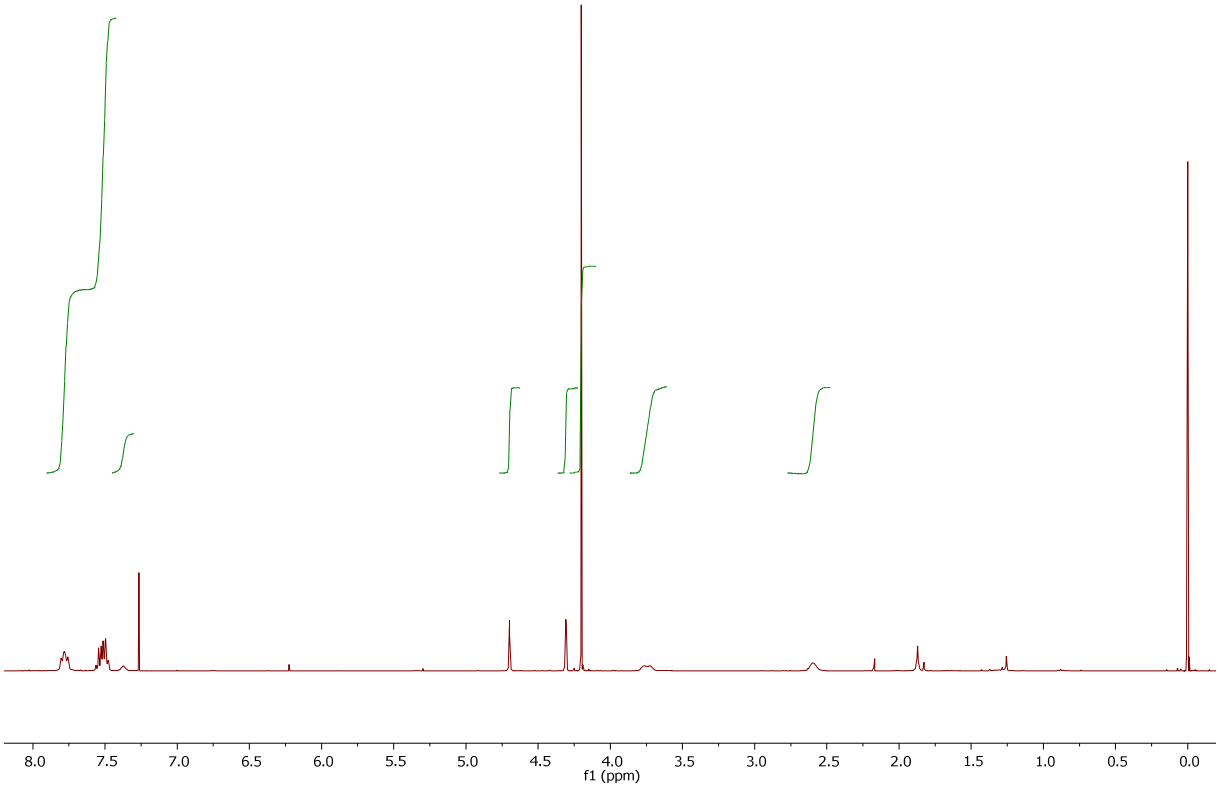

Figure S13. ^{1}H NMR (400 MHz, $CDCl_3$) spectrum of **1O**.

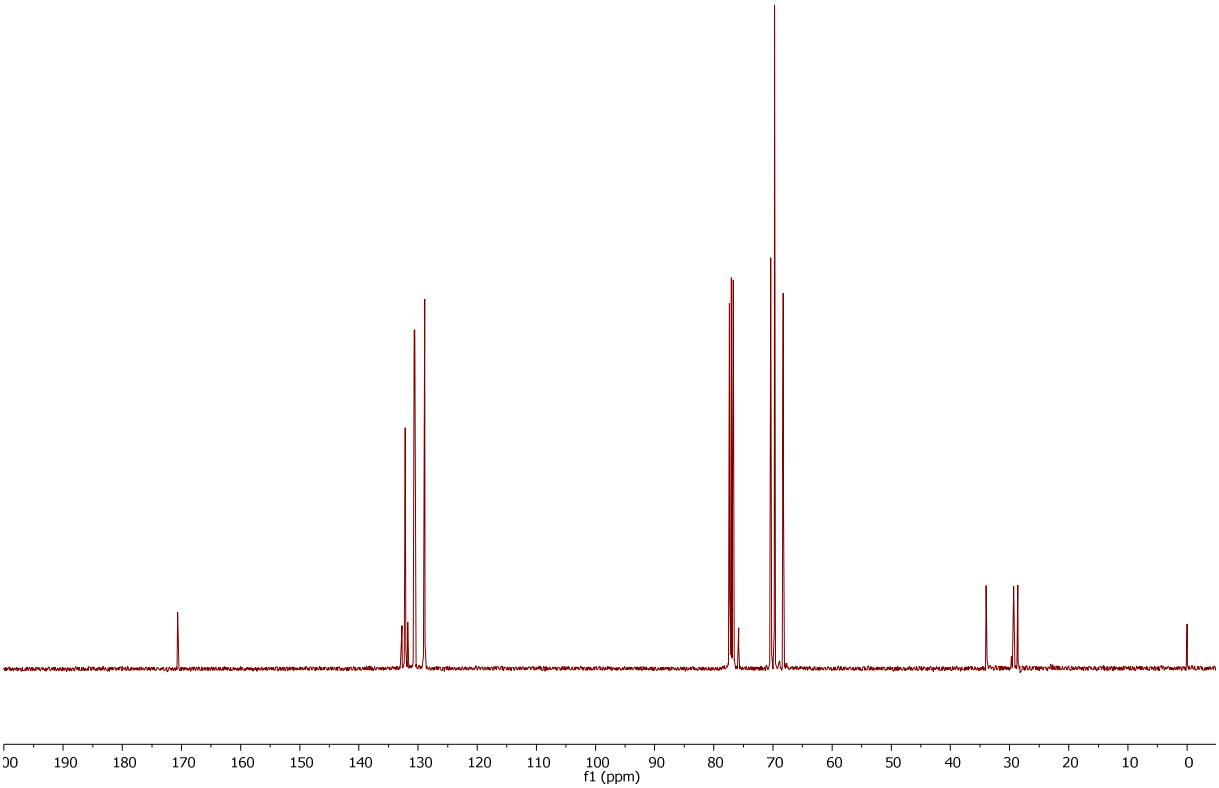

Figure S14. $^{13}C\{^{1}H\}$ NMR (101 MHz, $CDCl_3$) spectrum of **1O**.

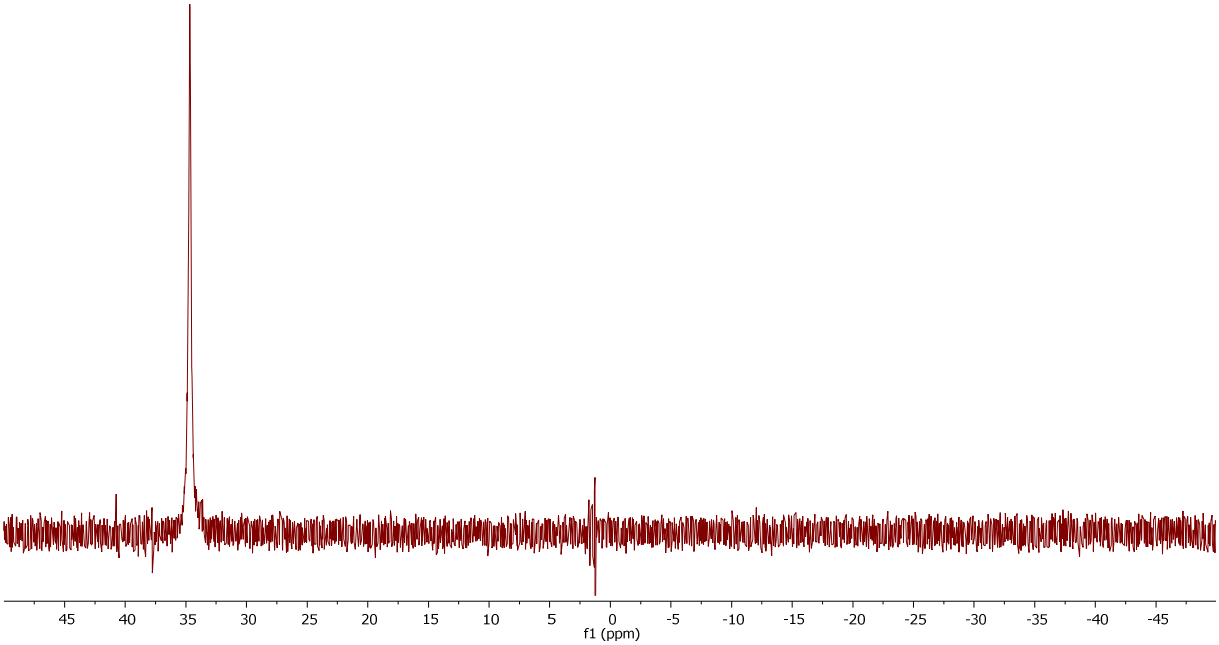

Figure S15. $^{31}P\{^{1}H\}$ NMR (162 MHz, $CDCl_3$) spectrum of **1O**.

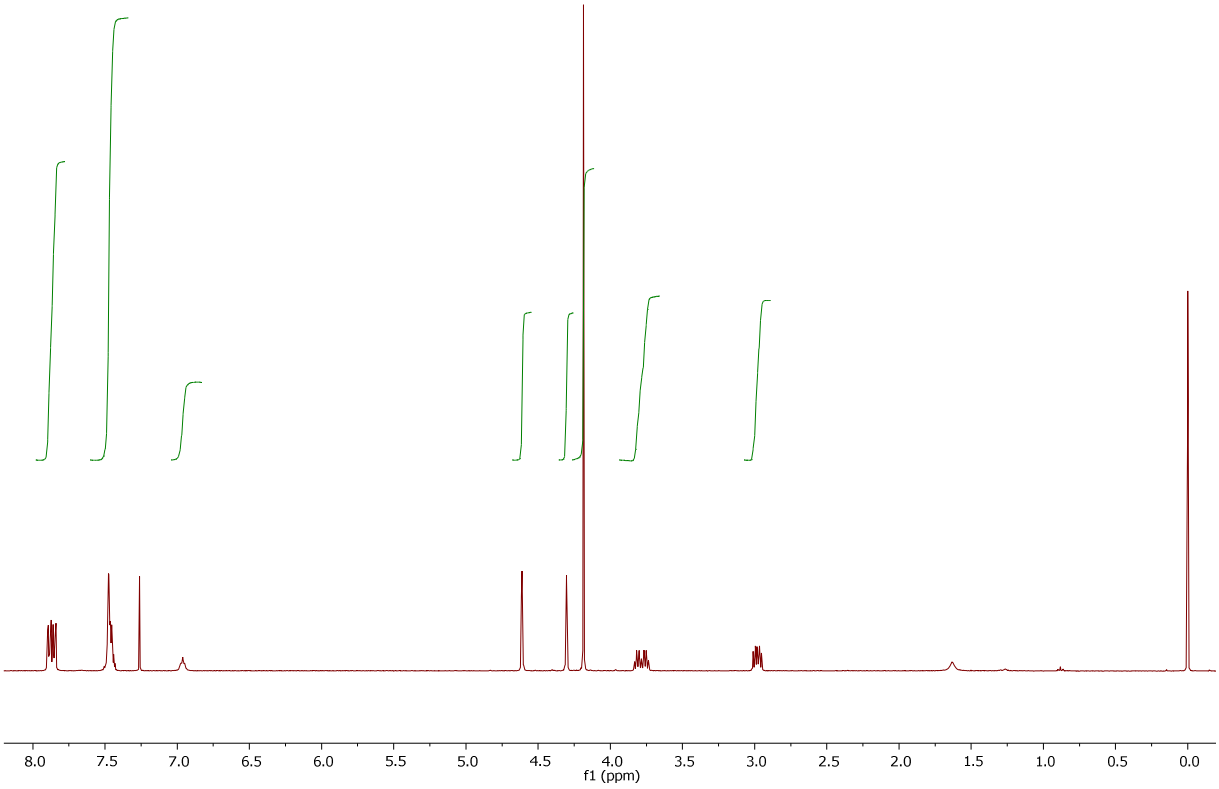

Figure S16. ^{1}H NMR (400 MHz, $CDCl_3$) spectrum of **1Se**.

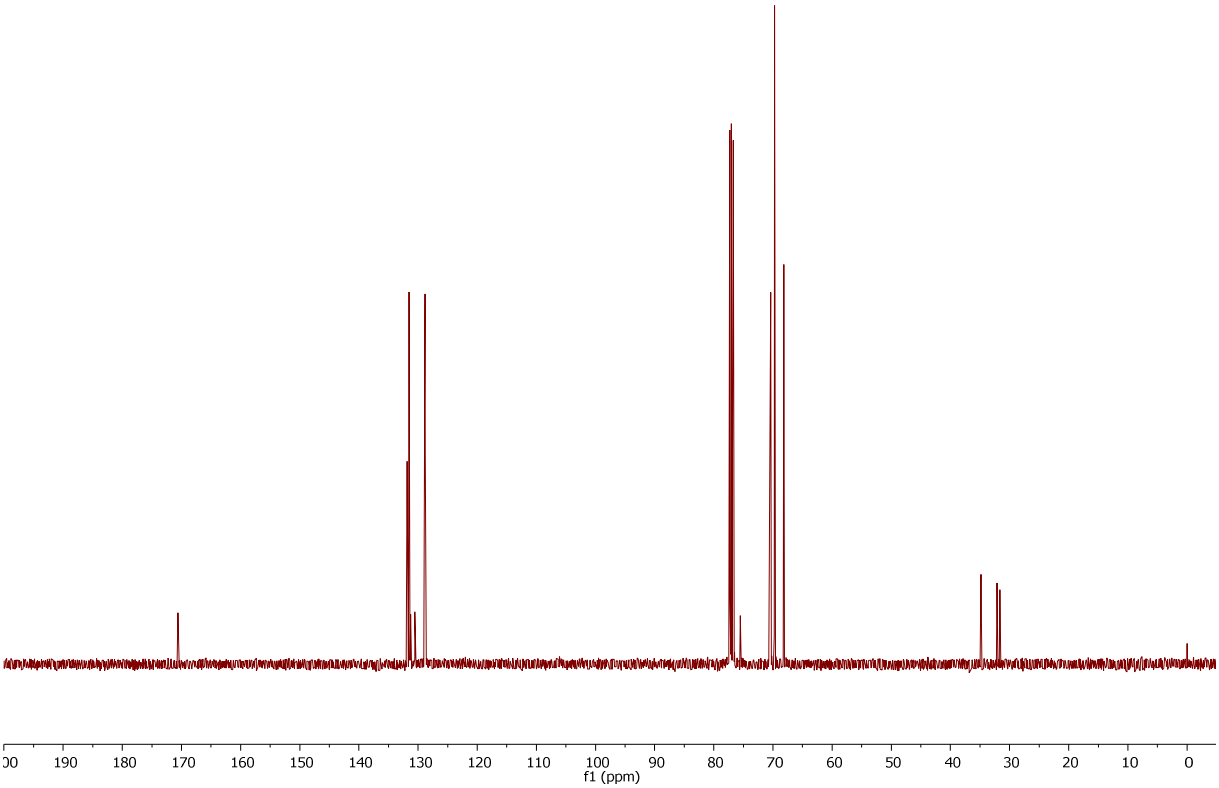

Figure S17. $^{13}C\{^{1}H\}$ NMR (101 MHz, $CDCl_3$) spectrum of **1Se**.

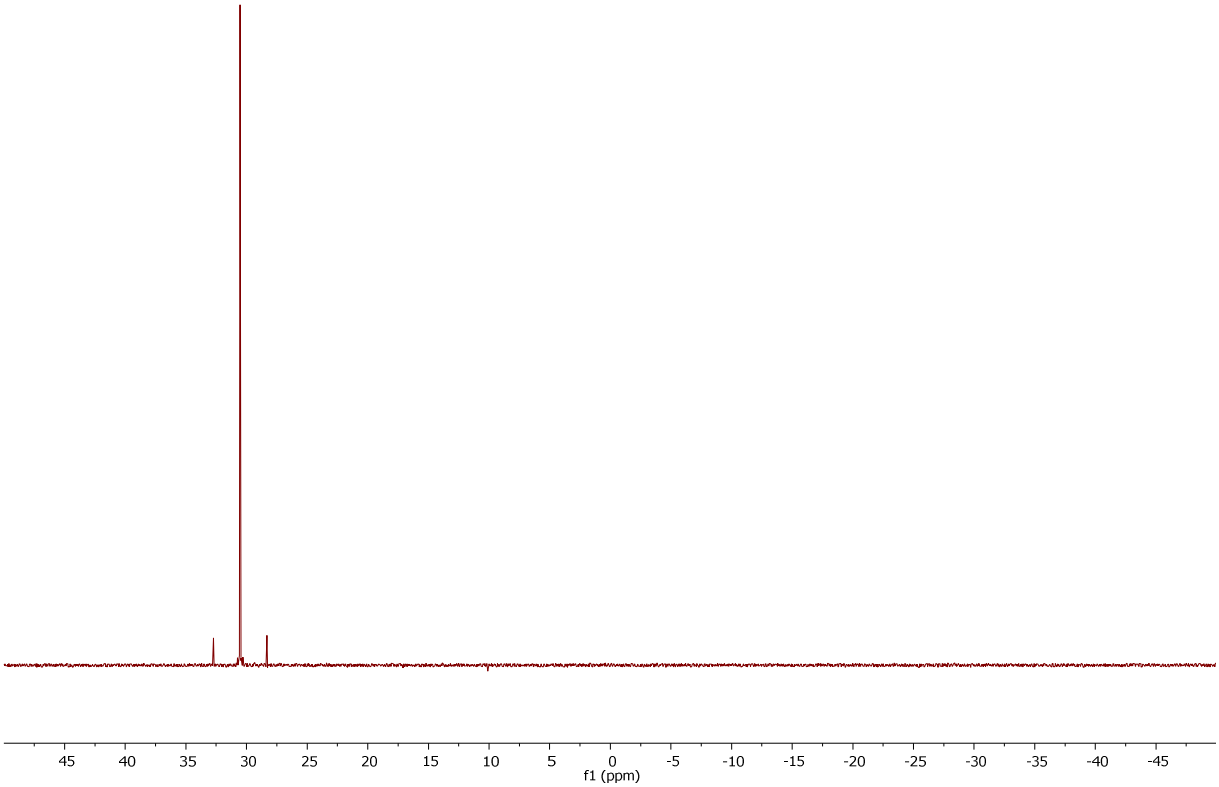

Figure S18. $^{31}P\{^{1}H\}$ NMR (162 MHz, $CDCl_3$) spectrum of **1Se**.

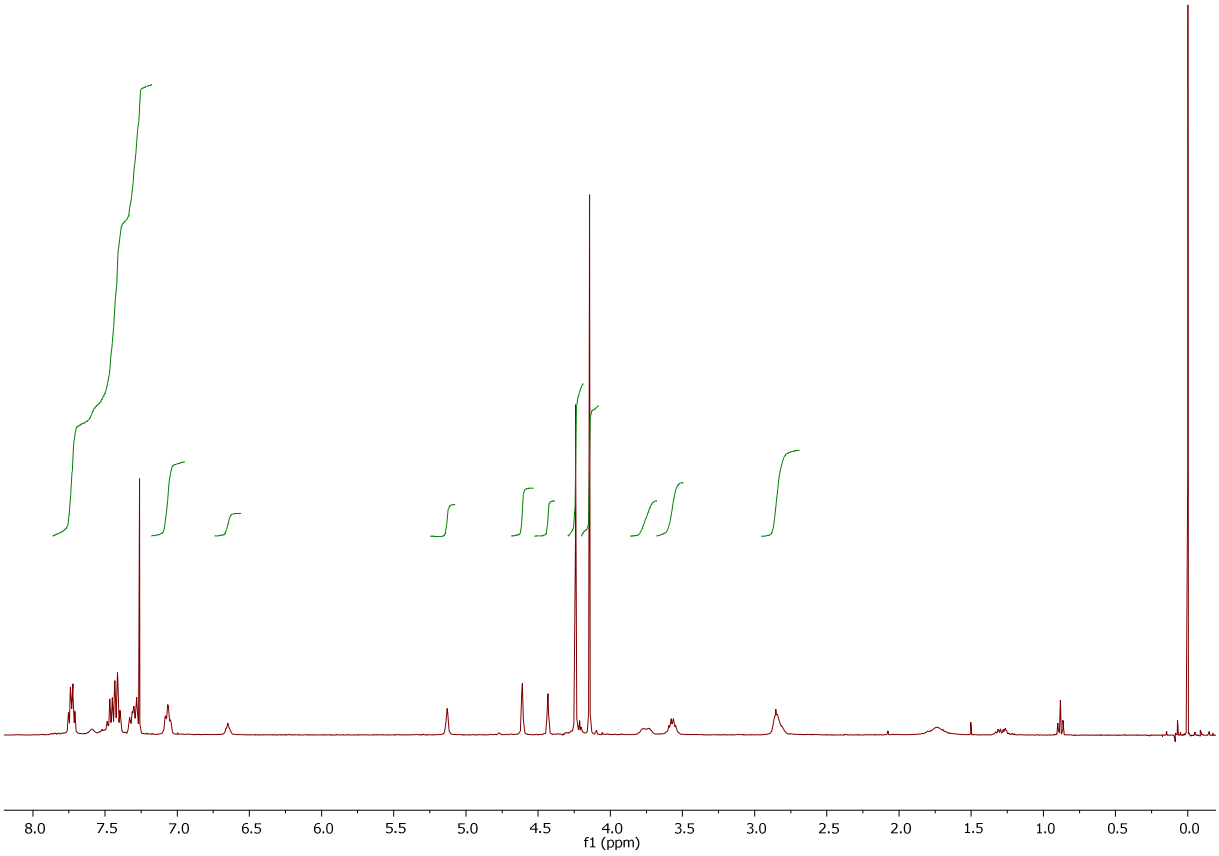

Figure S19. ^{1}H NMR (400 MHz, $CDCl_3$) spectrum of **2a** (mixture of isomers).

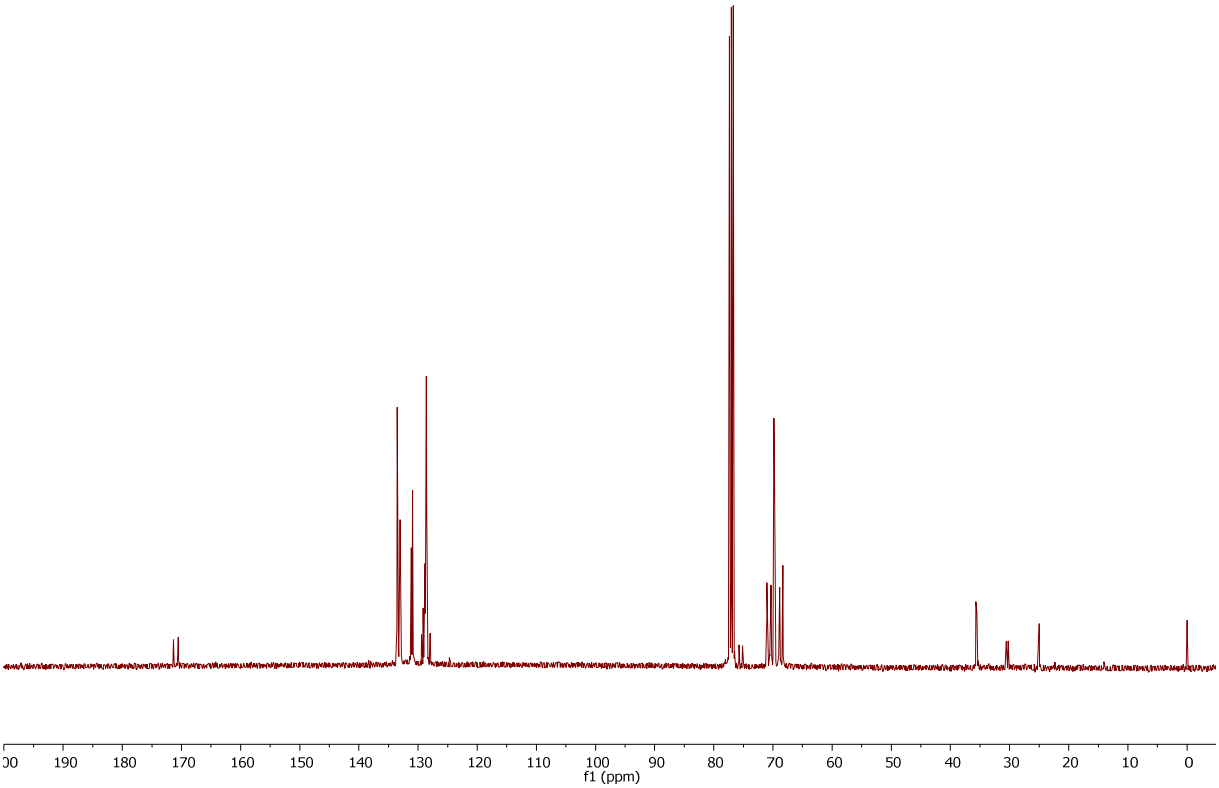

Figure S20. $^{13}C\{^{1}H\}$ NMR (101 MHz, $CDCl_3$) spectrum of **2a** (mixture of isomers).

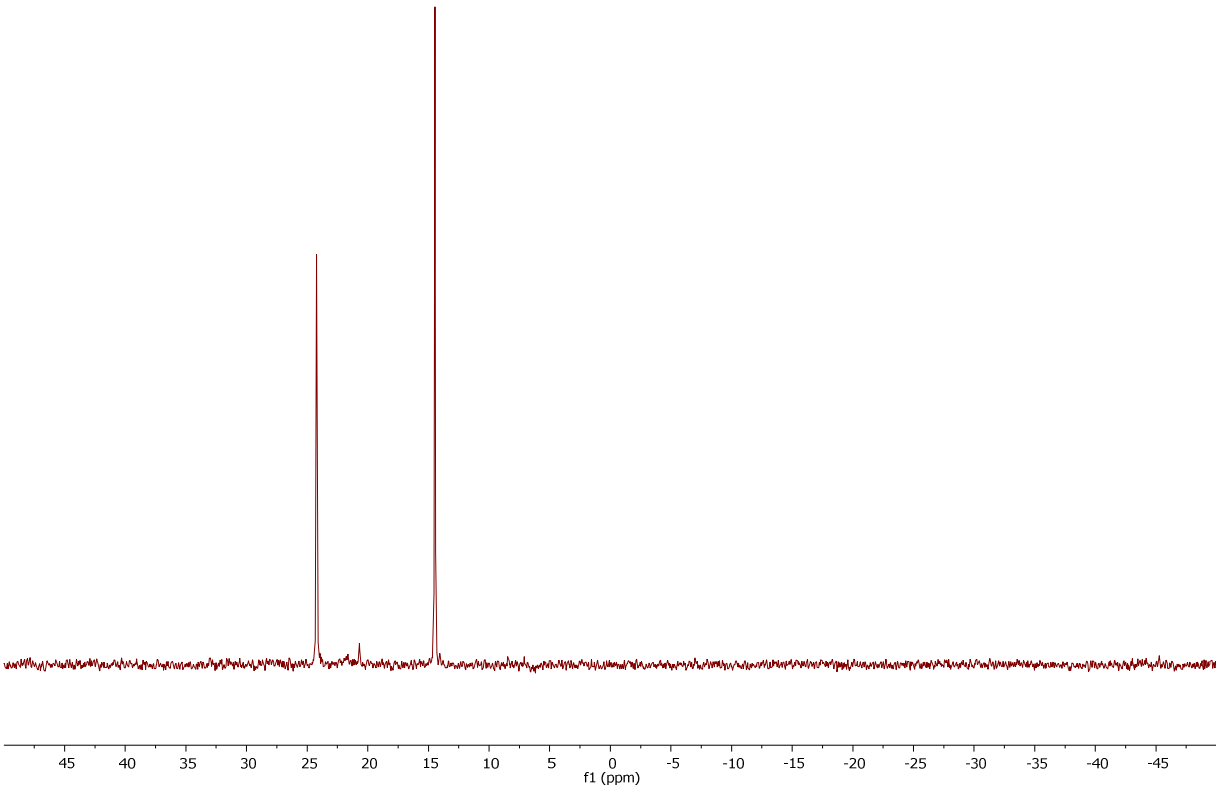

Figure S21. $^{31}P\{^{1}H\}$ NMR (162 MHz, $CDCl_3$) spectrum of **2a** (mixture of isomers).

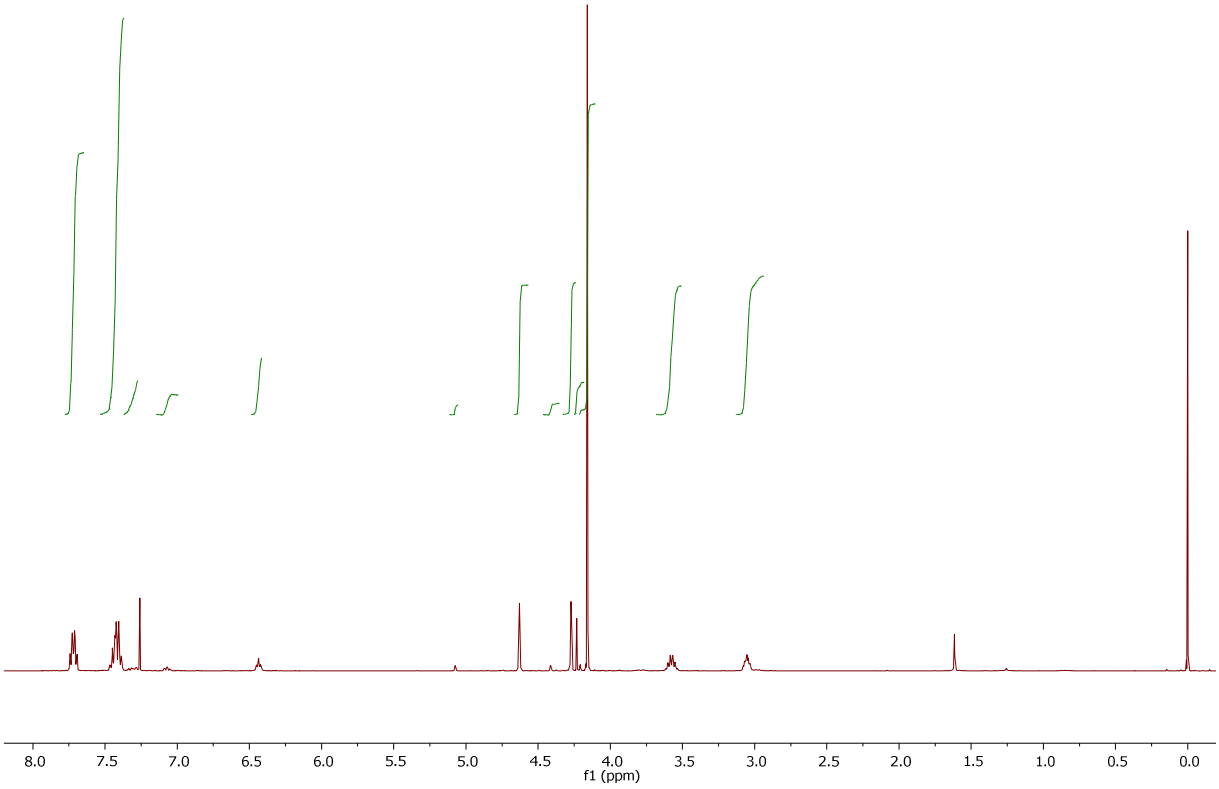

Figure 22. ^{1}H NMR (400 MHz, $CDCl_3$) spectrum of **2b** (mixture of isomers).

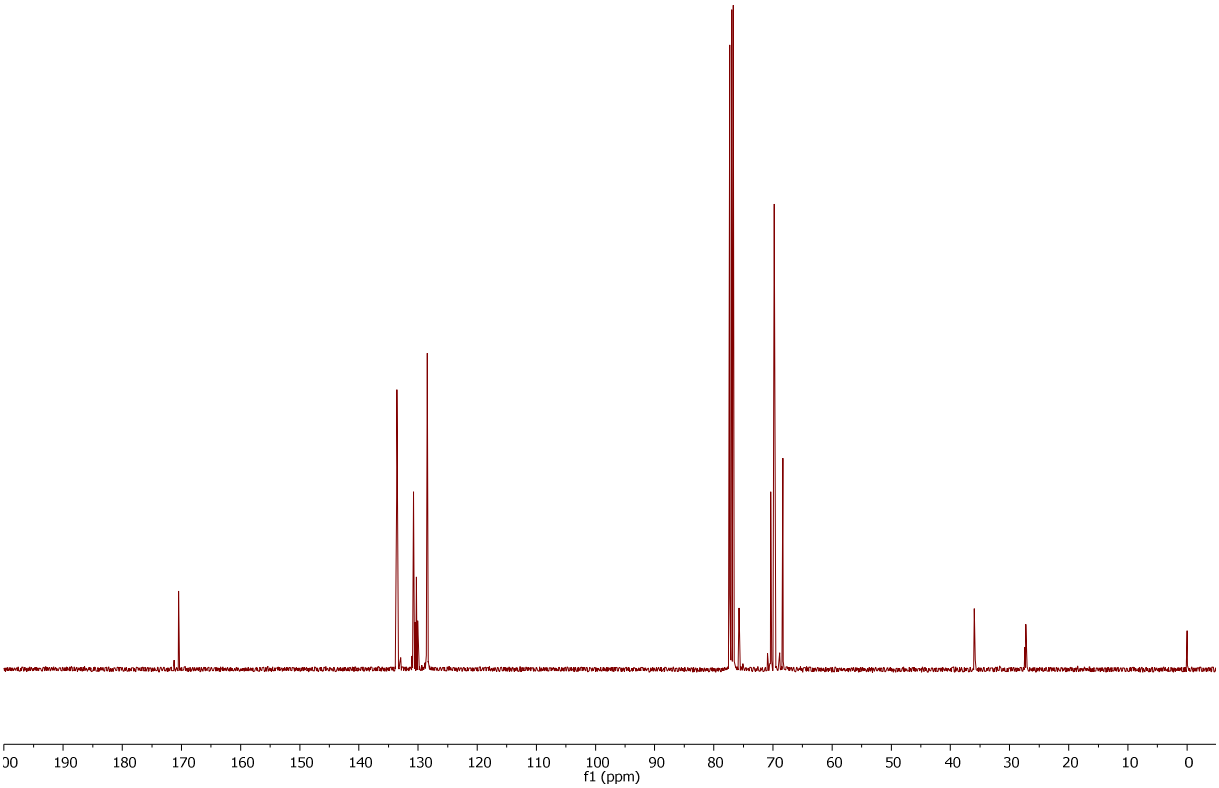

Figure S23. $^{13}C\{^{1}H\}$ NMR (101 MHz, $CDCl_3$) spectrum of **2b** (mixture of isomers).

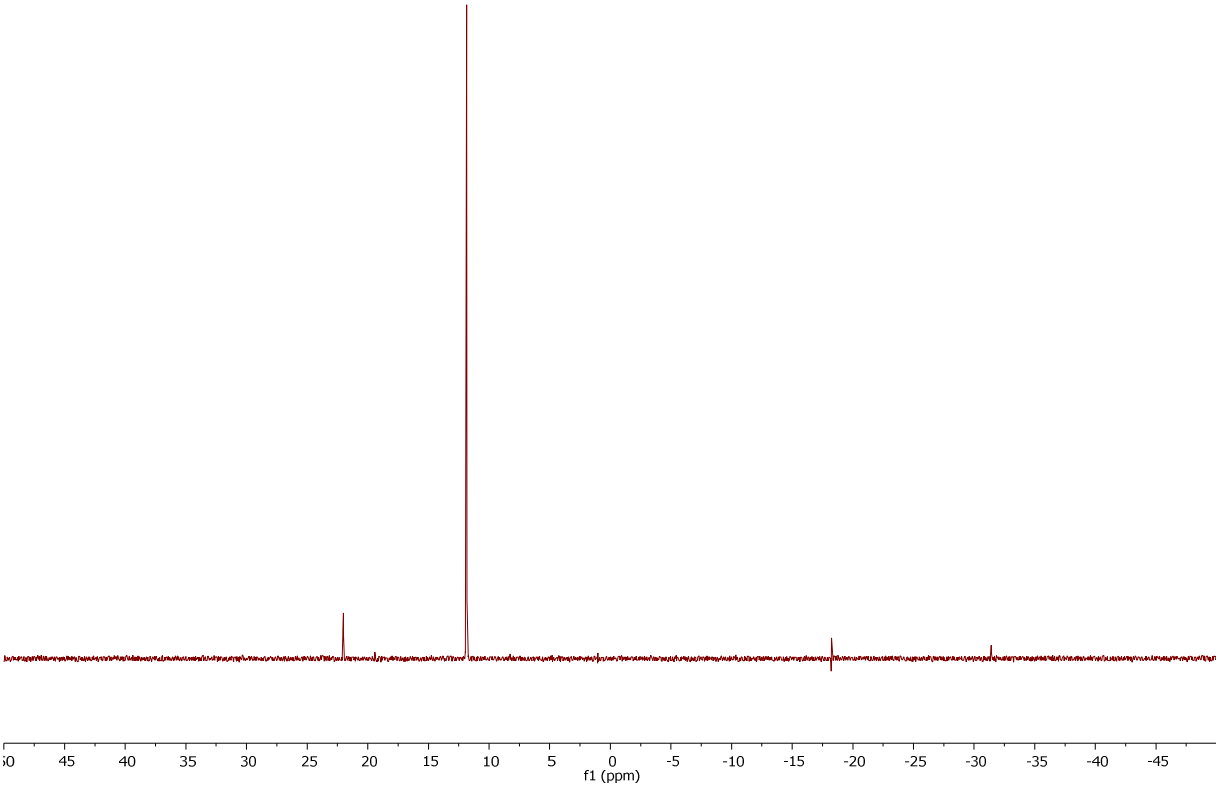

Figure S24. $^{31}P\{^{1}H\}$ NMR (162 MHz, $CDCl_3$) spectrum of **2b** (mixture of isomers).

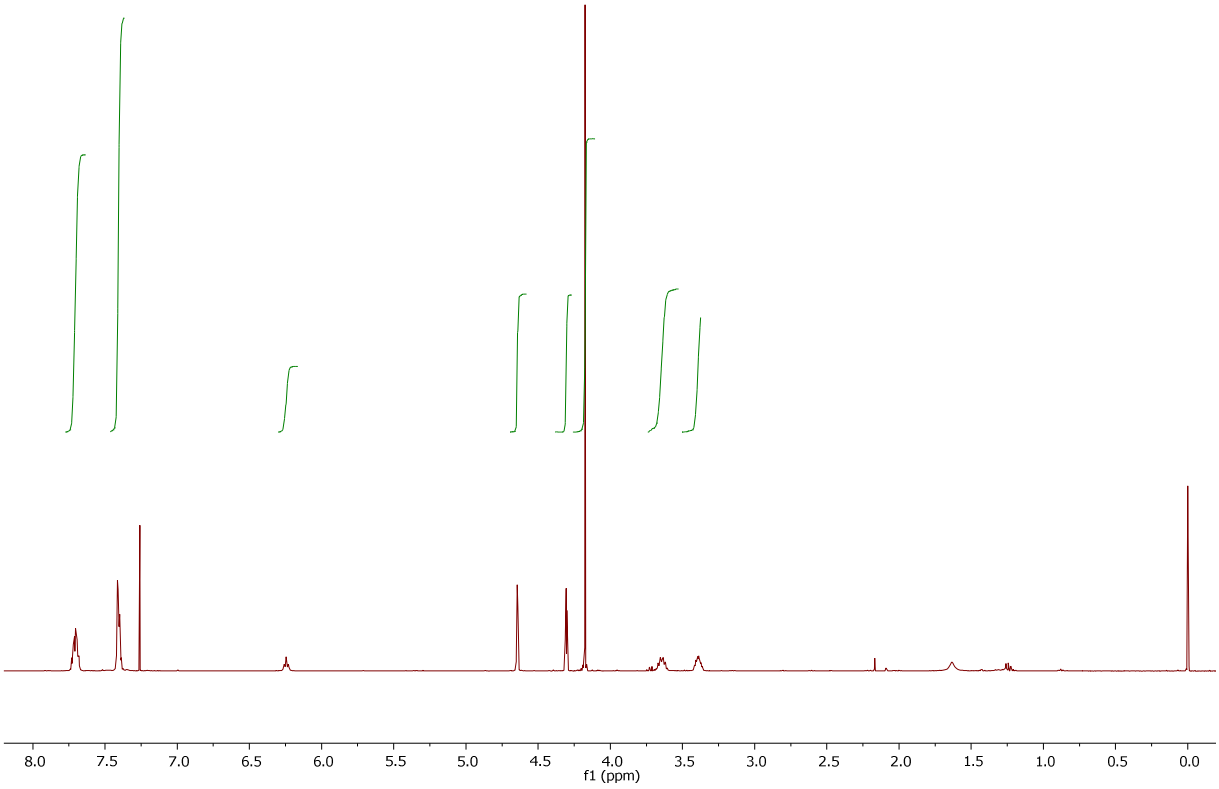

Figure S25. ^{1}H NMR (400 MHz, $CDCl_3$) spectrum of *trans*-**2c**.

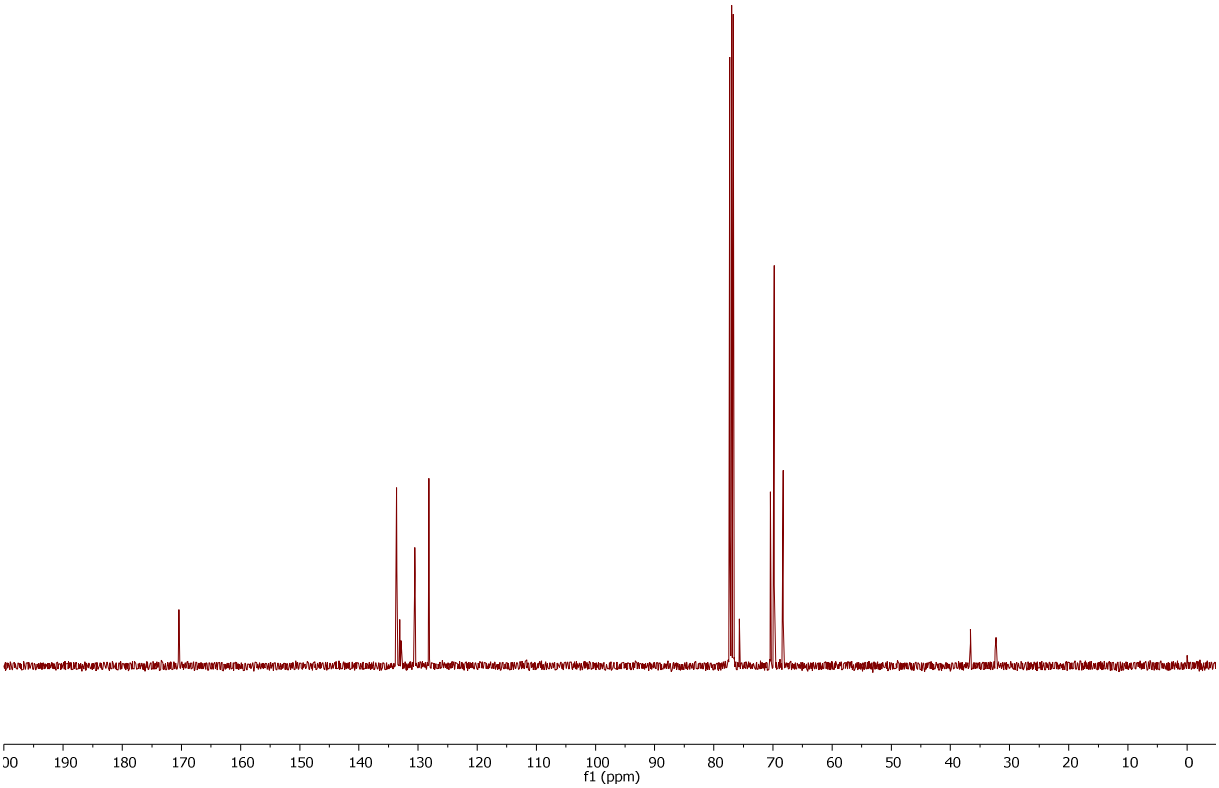

Figure S26. $^{13}C\{^{1}H\}$ NMR (101 MHz, $CDCl_3$) spectrum of *trans*-**2c**.

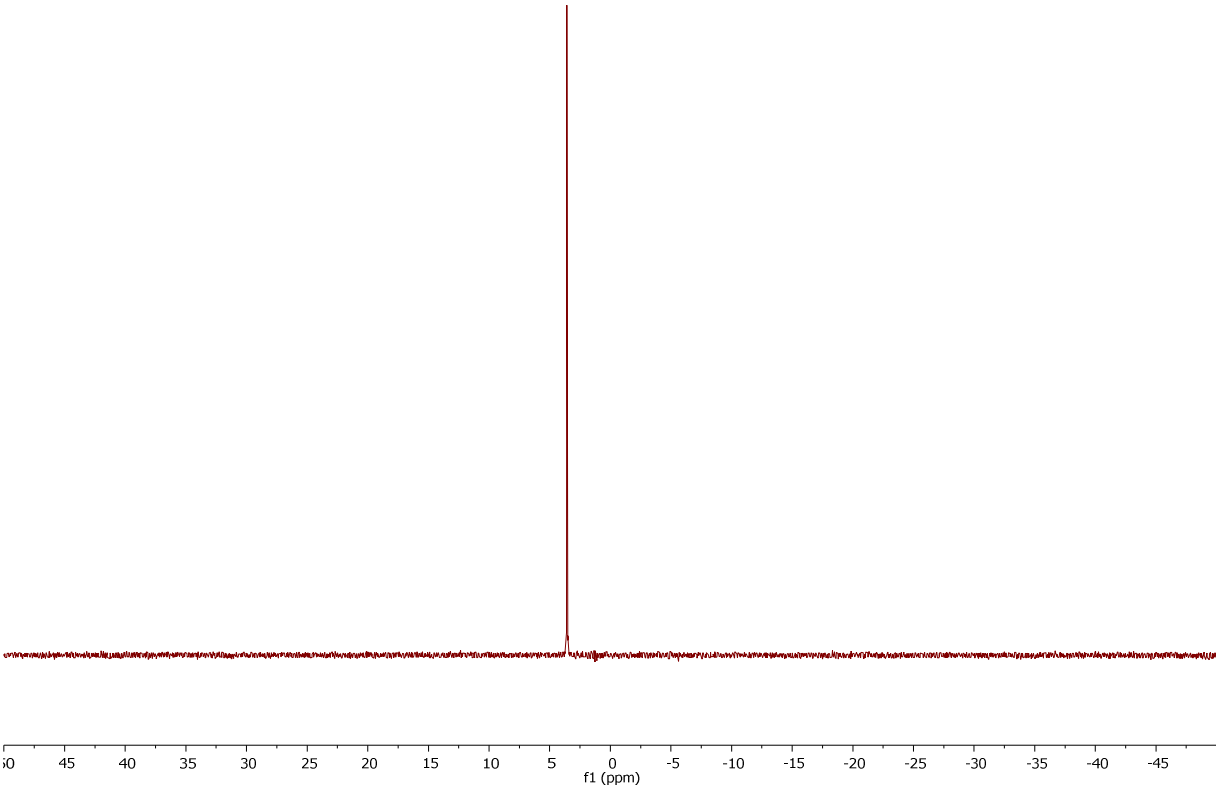

Figure S27. $^{31}P\{^{1}H\}$ NMR (162 MHz, $CDCl_3$) spectrum of *trans*-**2c**.

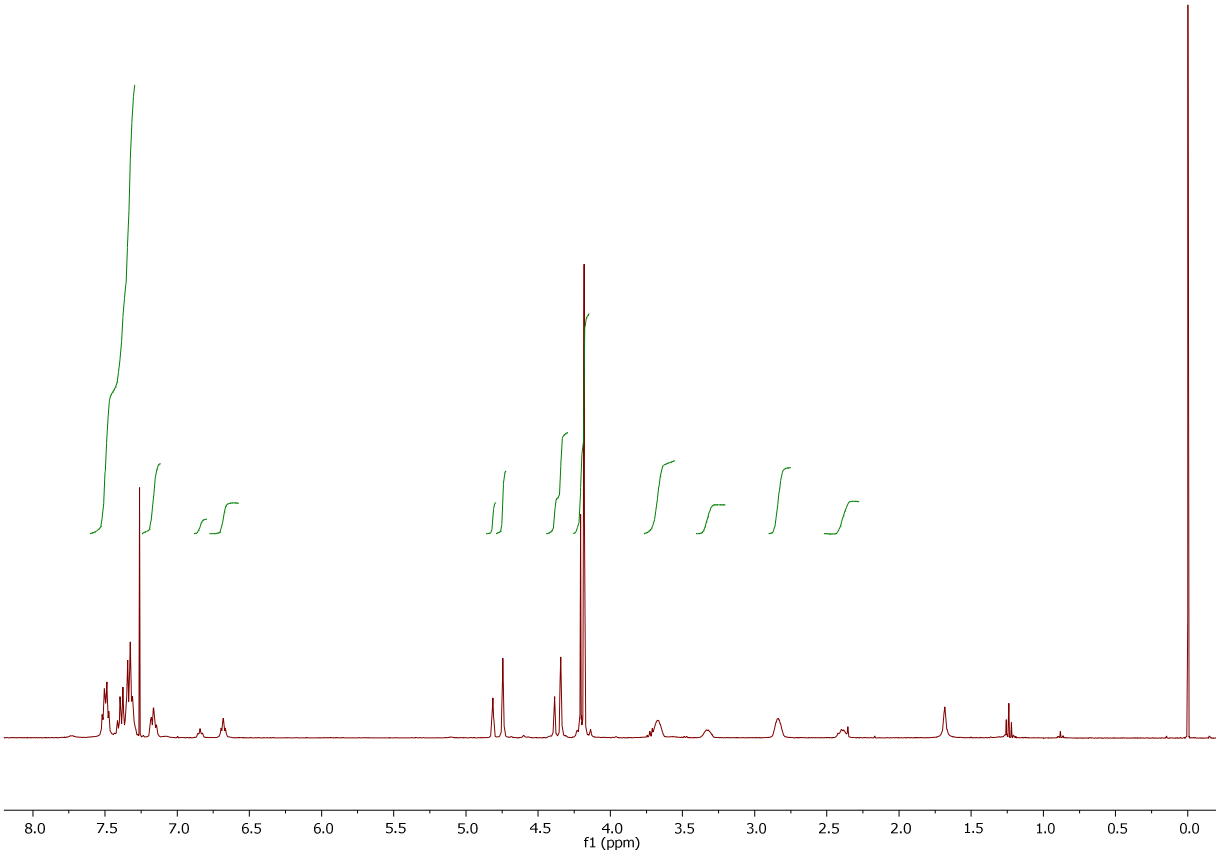

Figure S28. ^{1}H NMR (400 MHz, $CDCl_3$) spectrum of **3**.

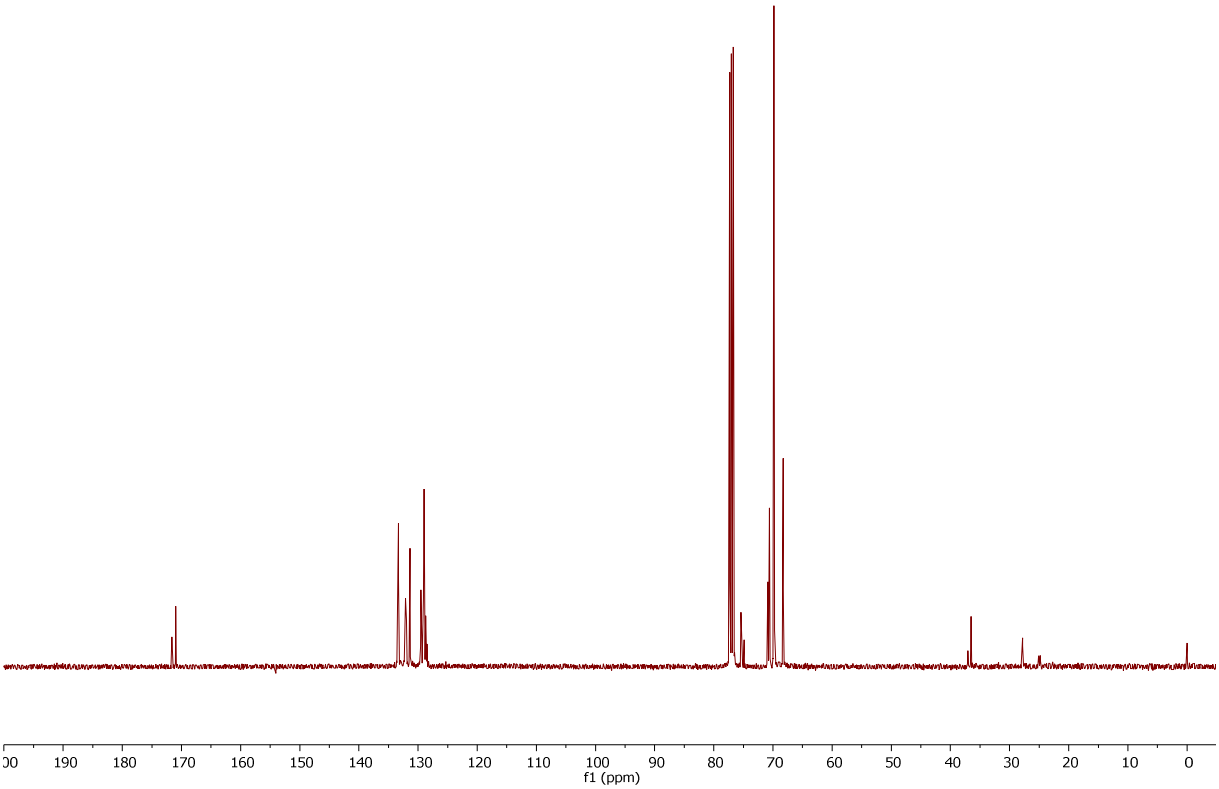

Figure S29. $^{13}C\{^{1}H\}$ NMR (101 MHz, $CDCl_3$) spectrum of **3**.

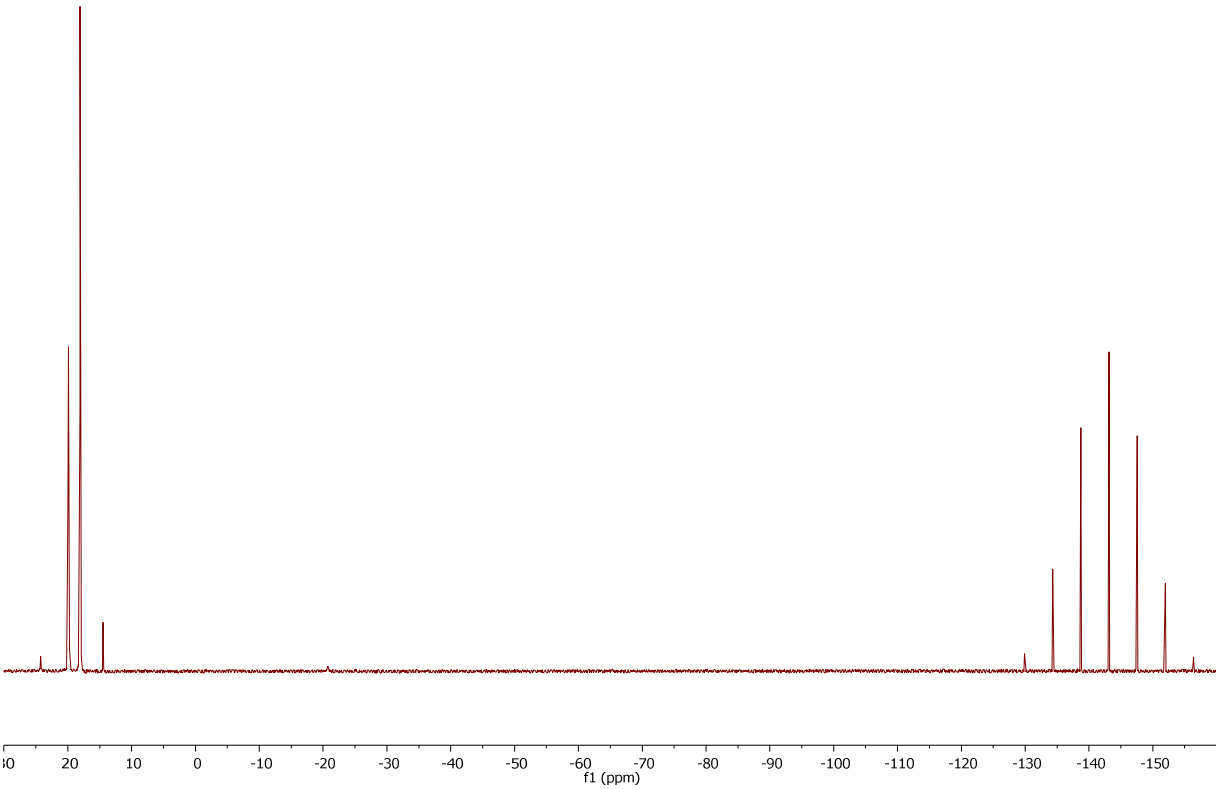

Figure S30. $^{31}P\{^{1}H\}$ NMR (162 MHz, $CDCl_3$) spectrum of **3**.

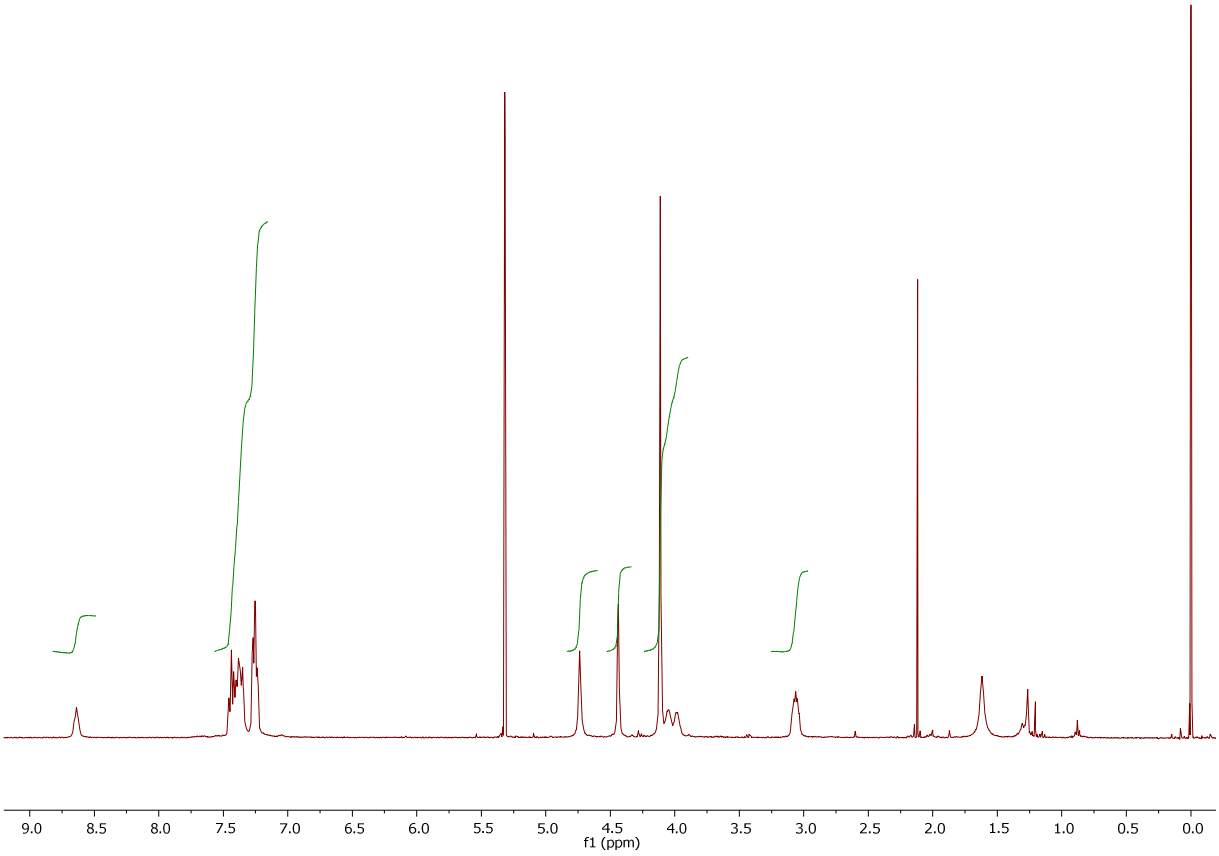

Figure S31. ^{1}H NMR (400 MHz, CD_2Cl_2) spectrum of **4a**.

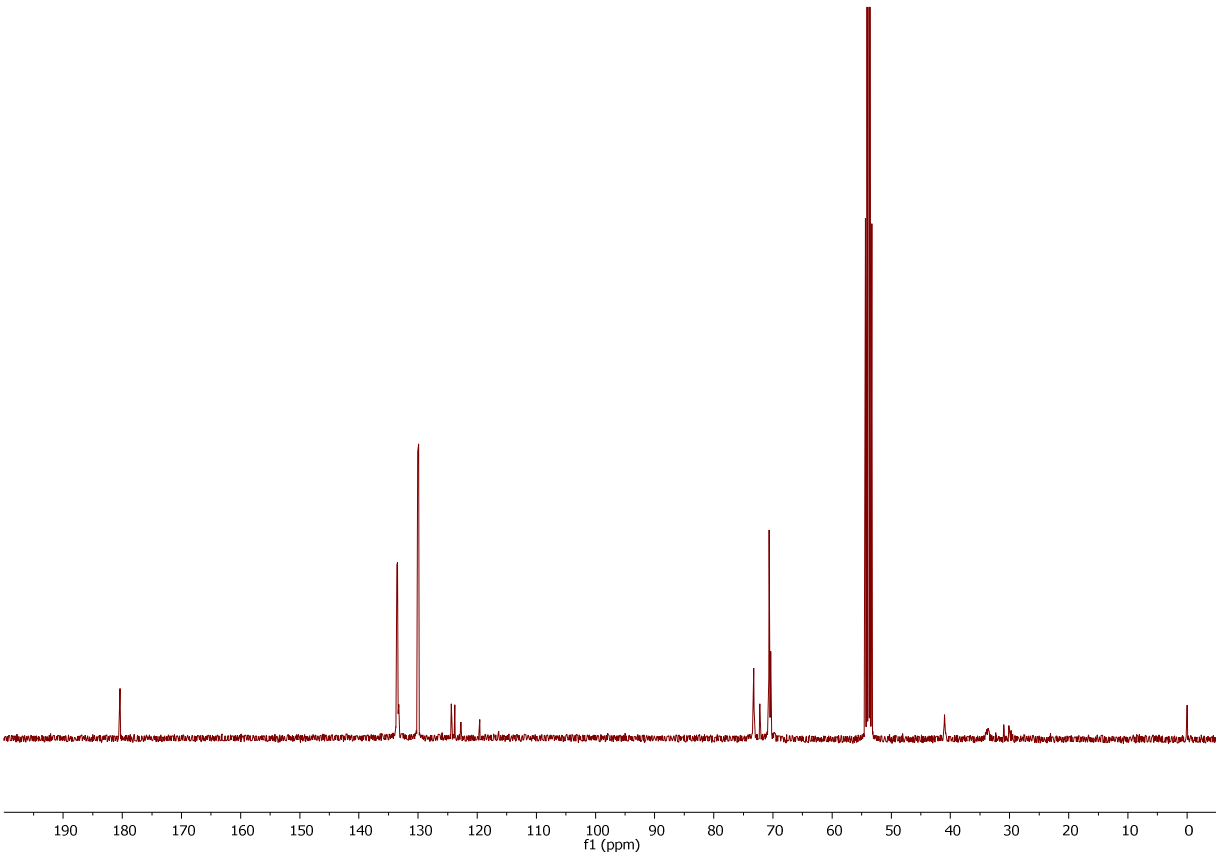

Figure S32. $^{13}C\{^{1}H\}$ NMR (101 MHz, CD_2Cl_2) spectrum of **4a**.

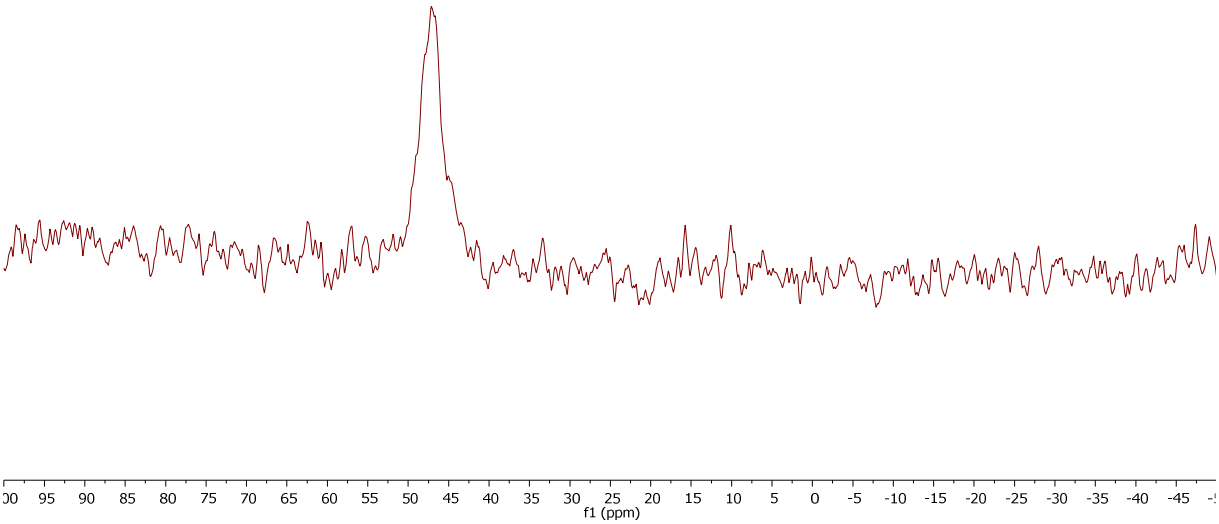

Figure S33. $^{31}P\{^{1}H\}$ NMR (162 MHz, CD_2Cl_2) spectrum of **4a**.

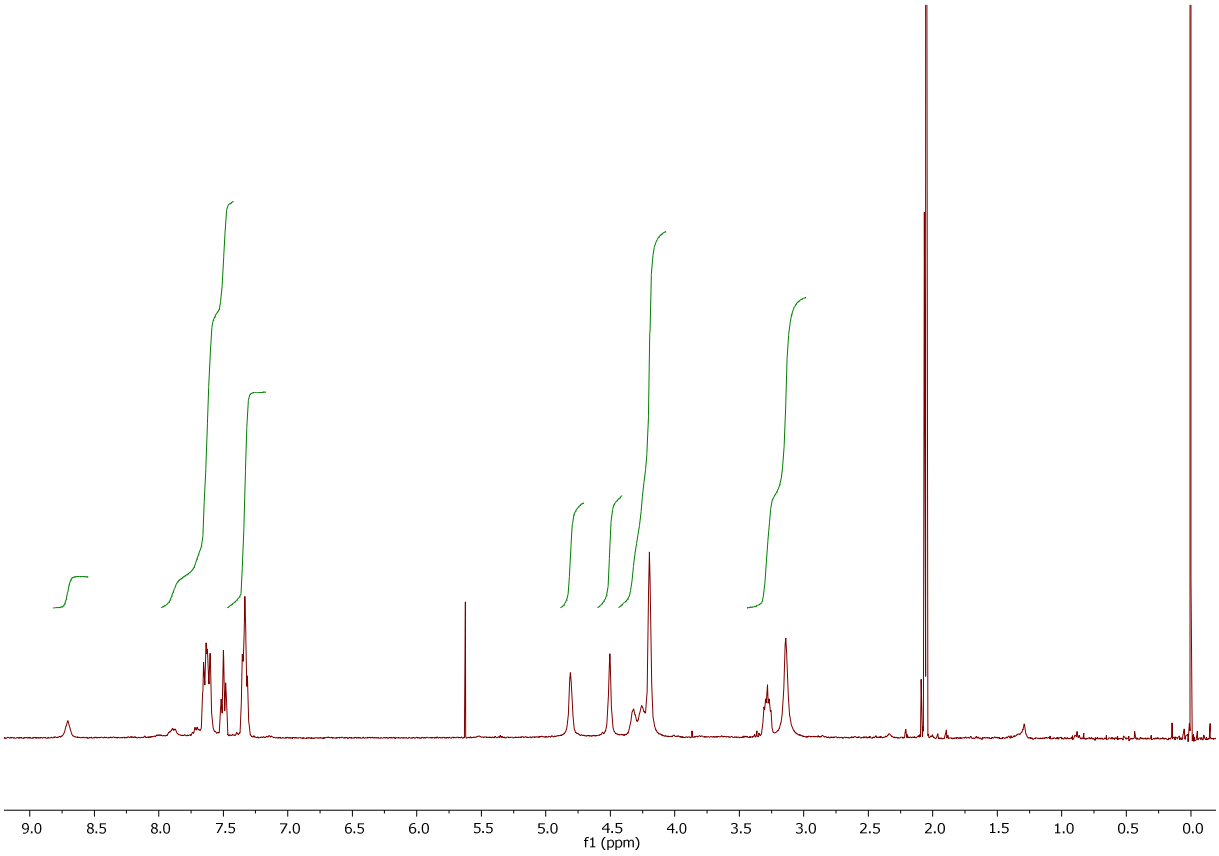

Figure S34. ^{1}H NMR (400 MHz, CD_3COCH_3) spectrum of **4b**.

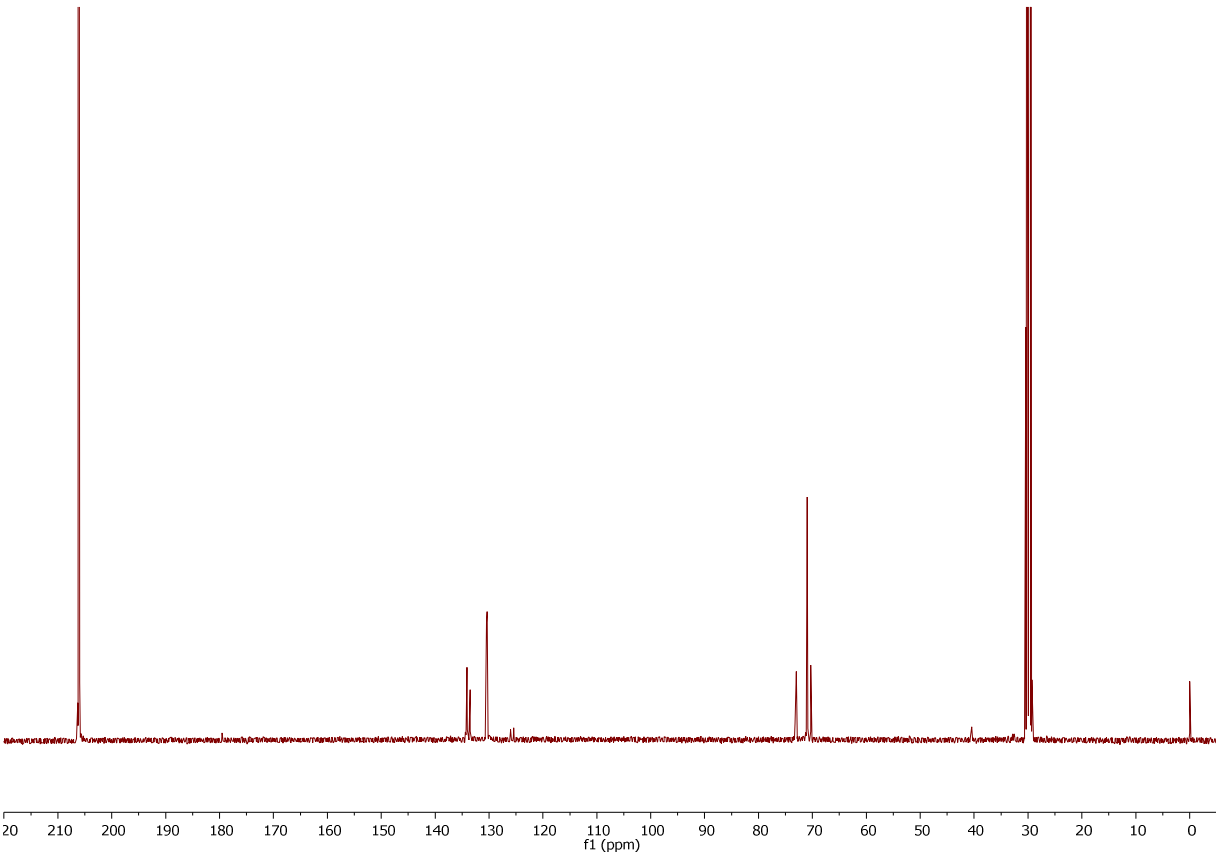

Figure S35. $^{13}C\{^{1}H\}$ NMR (101 MHz, CD_3COCH_3) spectrum of **4b**.

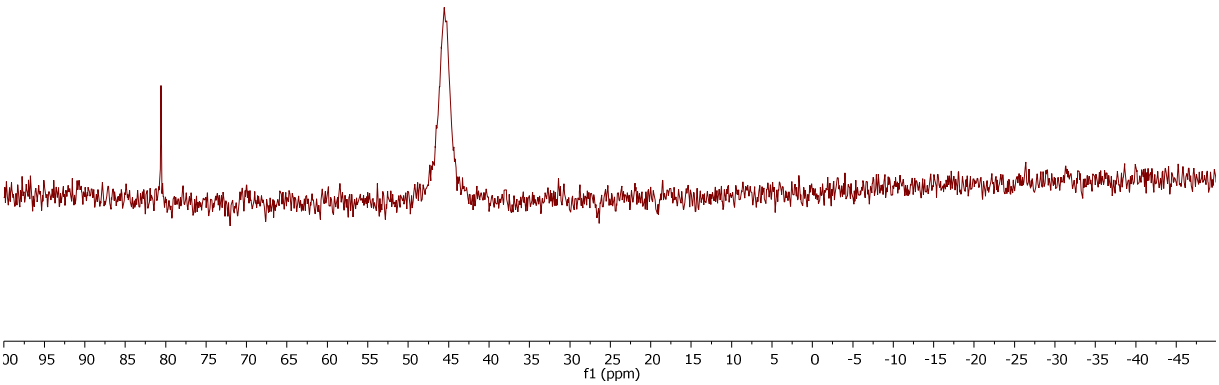

Figure S36. $^{31}P\{^{1}H\}$ NMR (162 MHz, CD_3COCH_3) spectrum of **4b**.

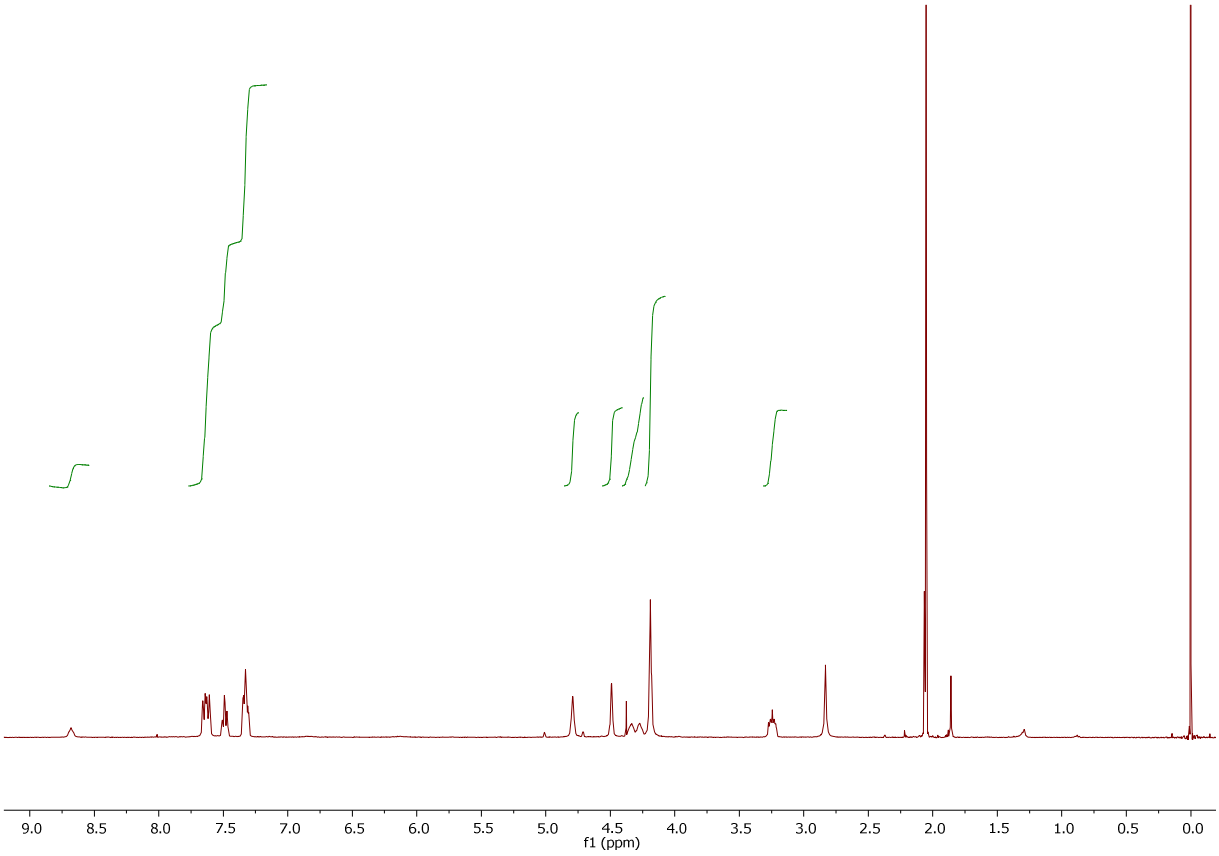

Figure S37. ^{1}H NMR (400 MHz, CD_3COCH_3) spectrum of **4c**.

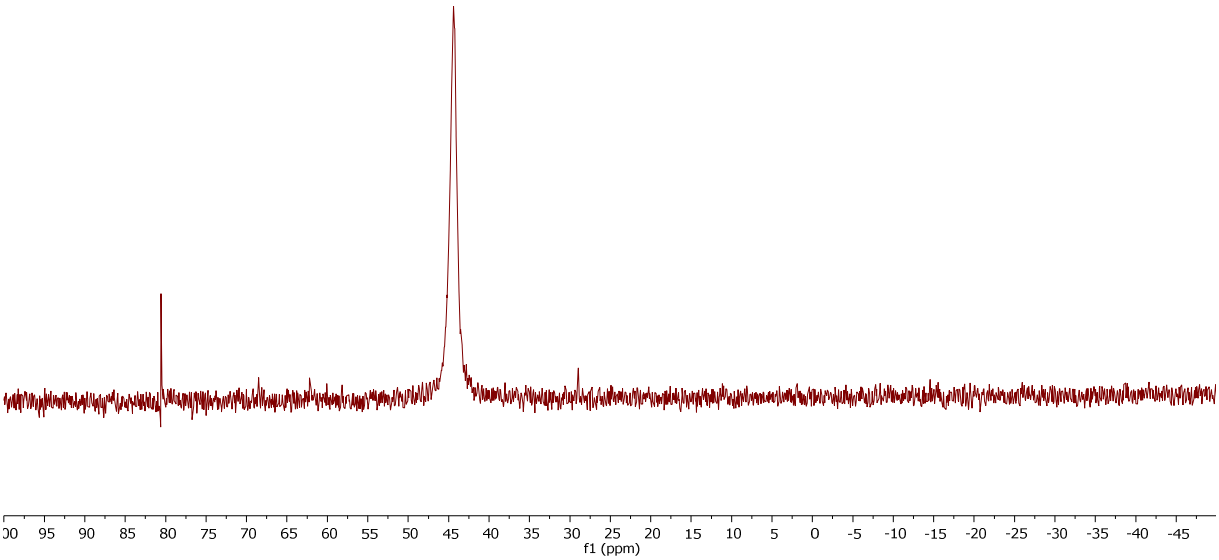

Figure S38. $^{31}P\{^{1}H\}$ NMR (162 MHz, CD_3COCH_3) spectrum of **4c**.

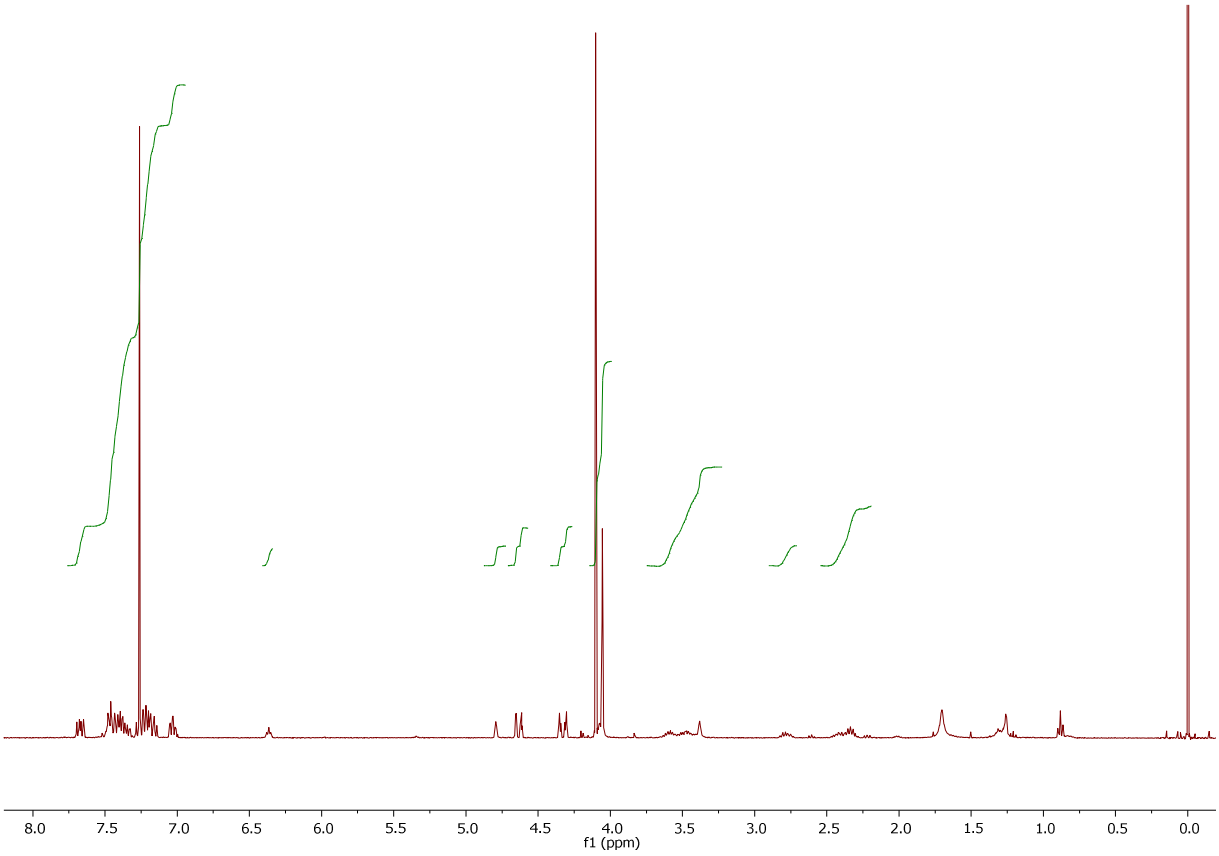

Figure S39. ^{1}H NMR (400 MHz, $CDCl_3$) spectrum of **5**.

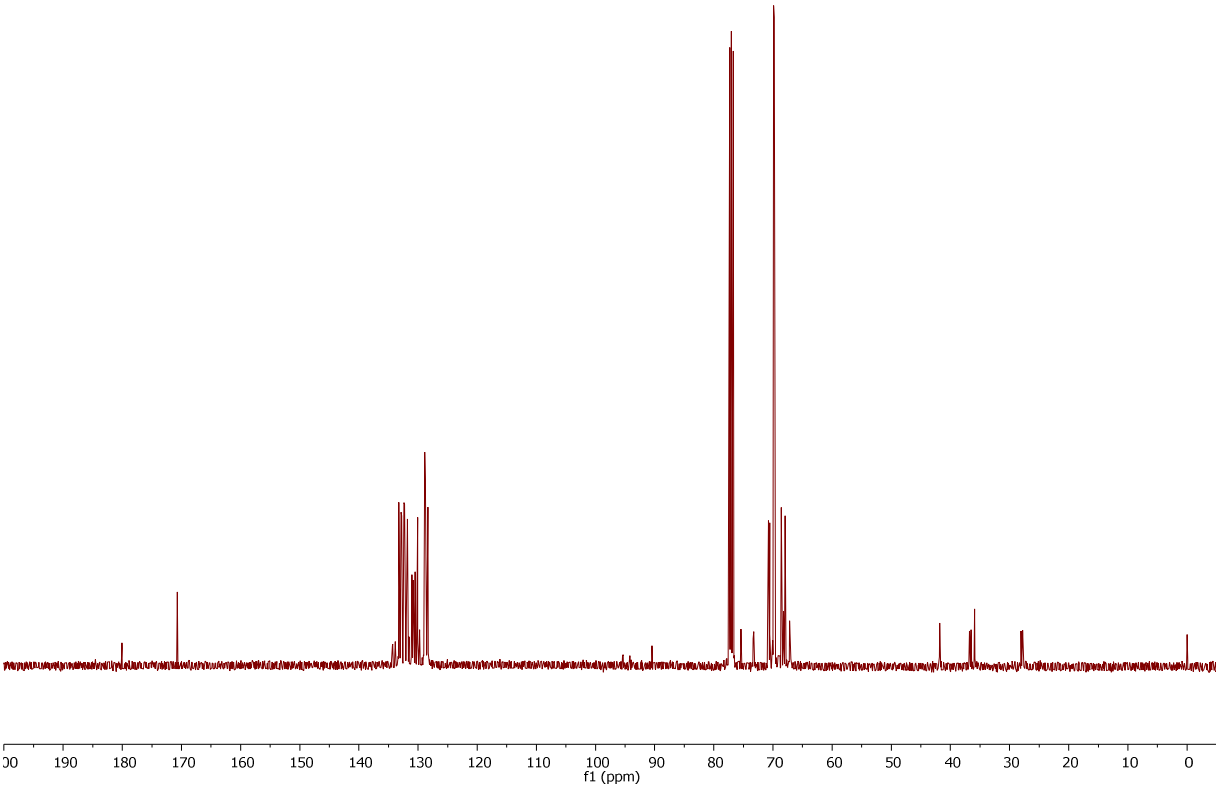

Figure S40. $^{13}C\{^{1}H\}$ NMR (101 MHz, $CDCl_3$) spectrum of **5**.

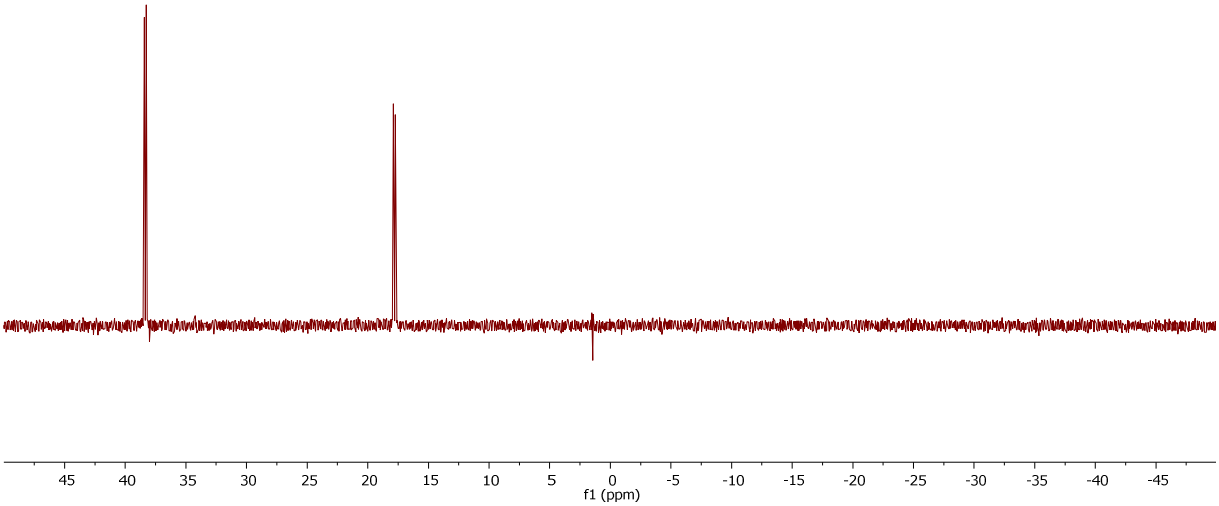

Figure S41. $^{31}P\{^{1}H\}$ NMR (162 MHz, $CDCl_3$) spectrum of **5**.

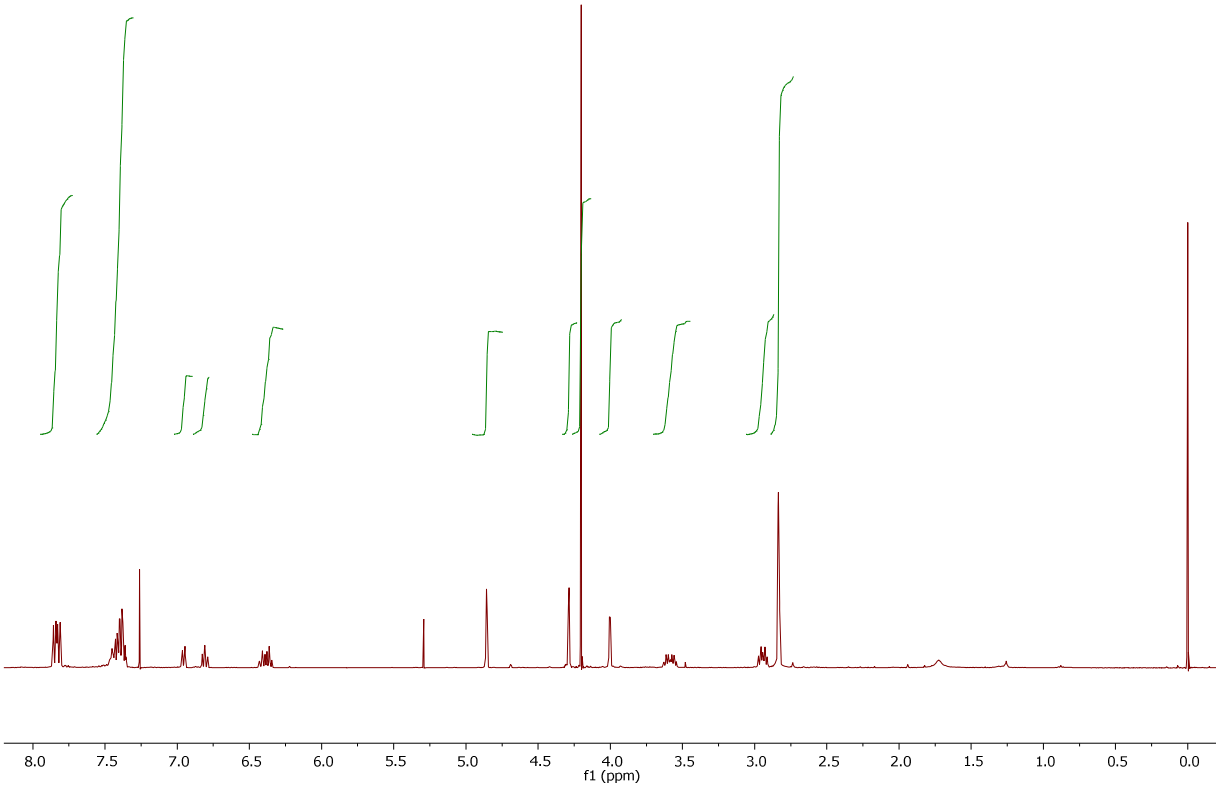

Figure S42. ^{1}H NMR (400 MHz, $CDCl_3$) spectrum of **6**.

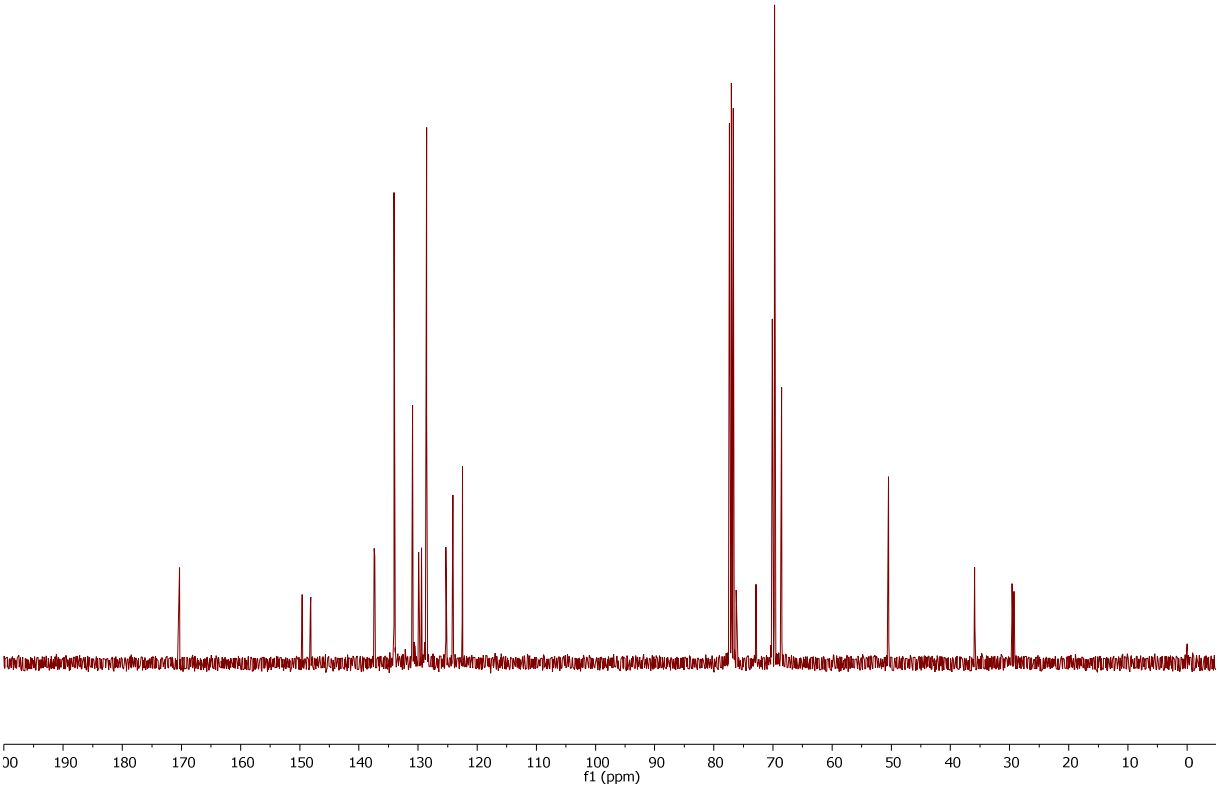

Figure S43. $^{13}C\{^{1}H\}$ NMR (101 MHz, $CDCl_3$) spectrum of **6**.

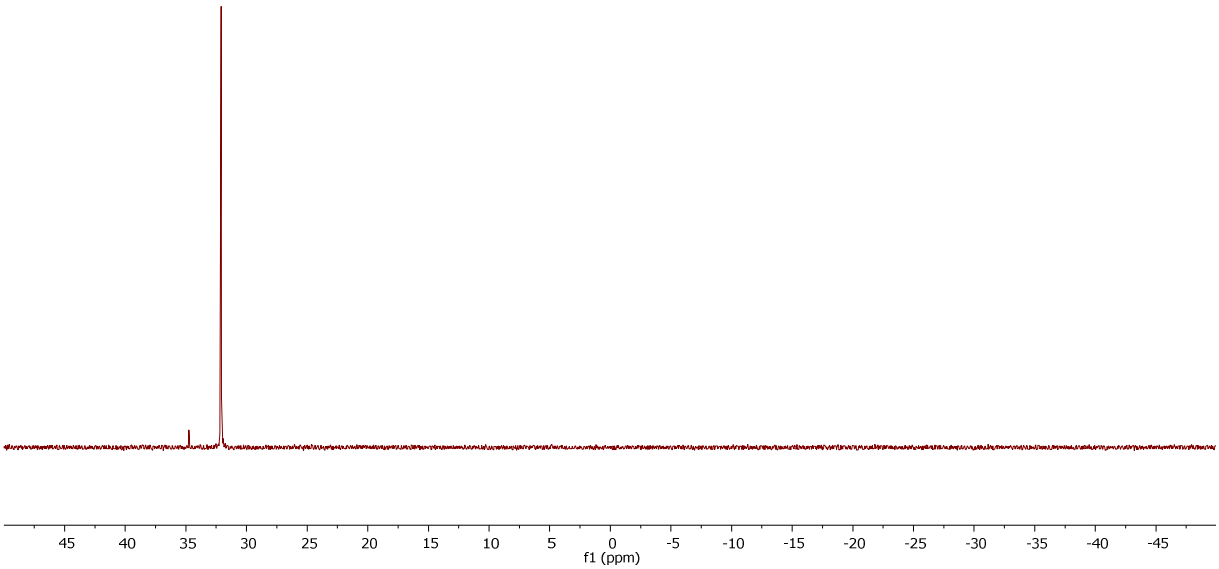

Figure S44. $^{31}P\{^{1}H\}$ NMR (162 MHz, $CDCl_3$) spectrum of **6**.

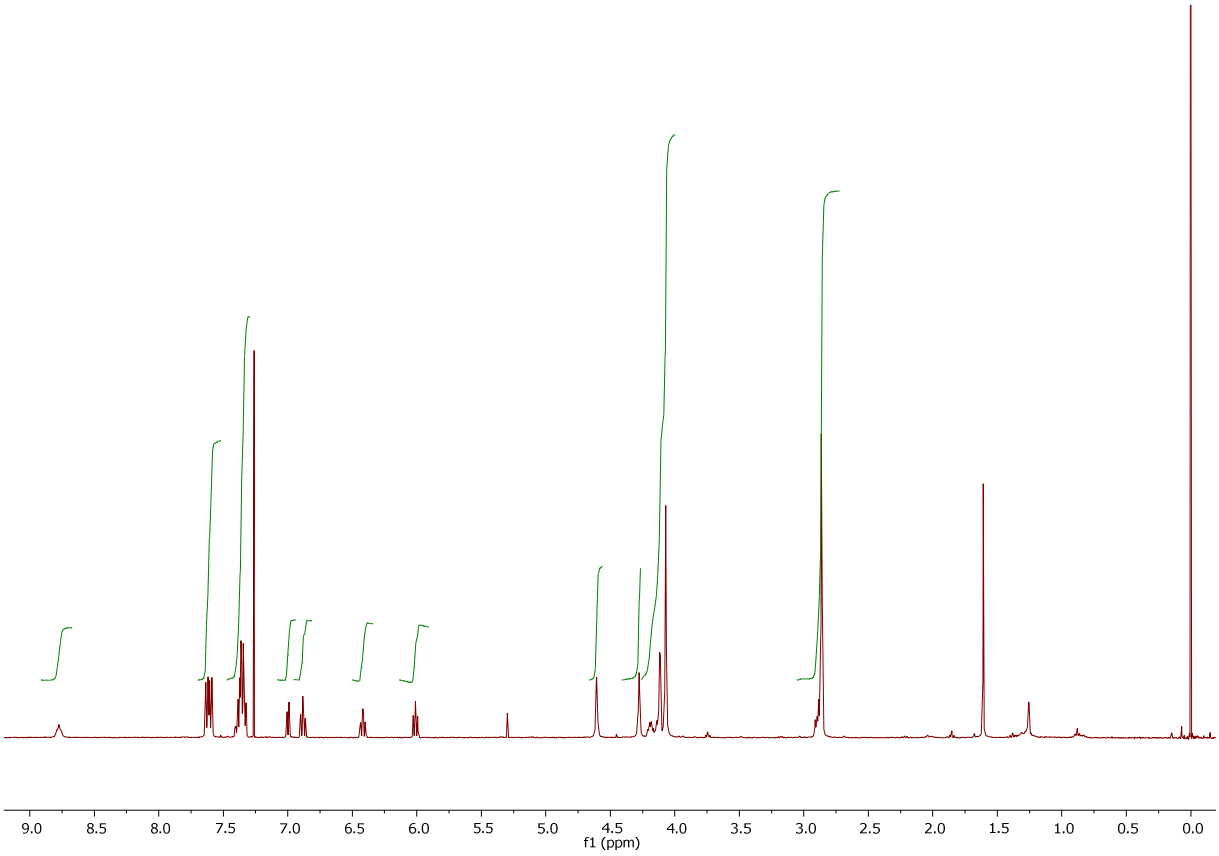

Figure S45. ^{1}H NMR (400 MHz, $CDCl_3$) spectrum of **7a**.

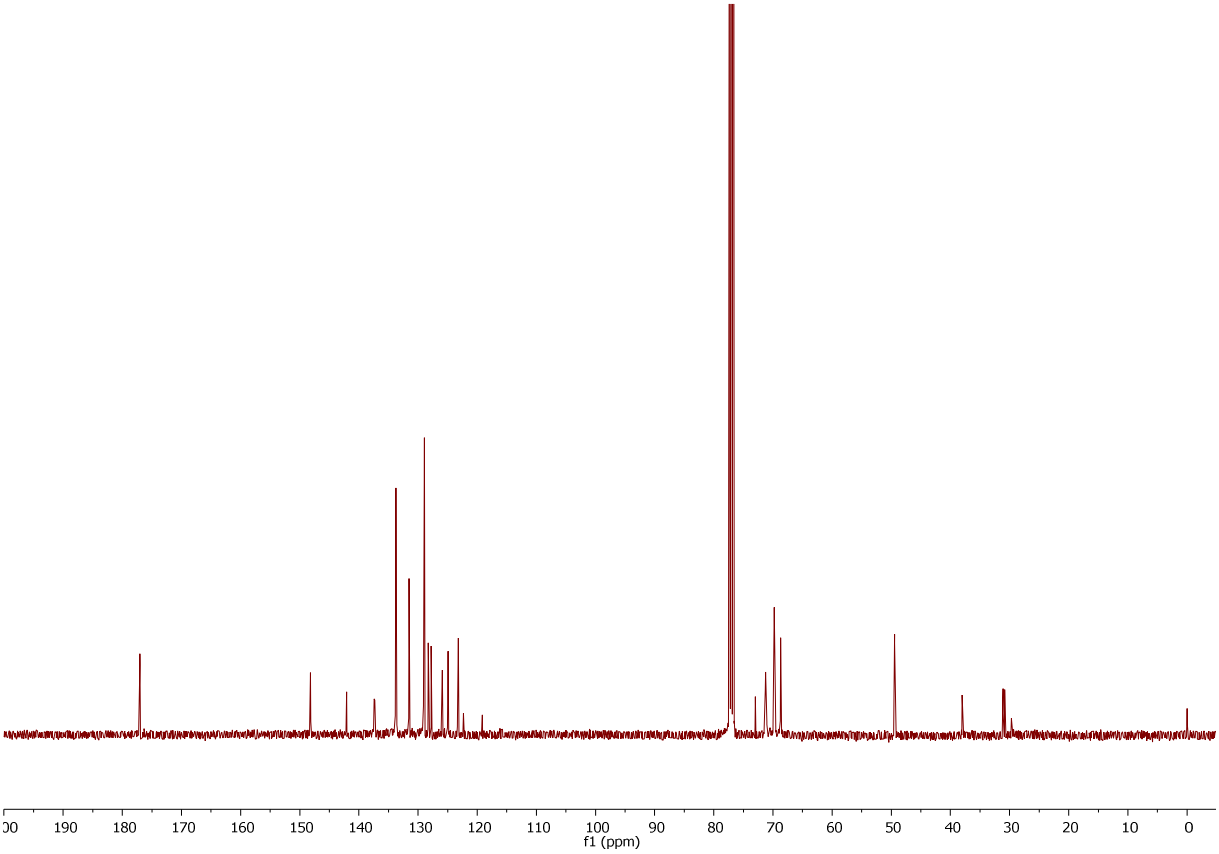

Figure S46. $^{13}C\{^{1}H\}$ NMR (101 MHz, $CDCl_3$) spectrum of **7a**.

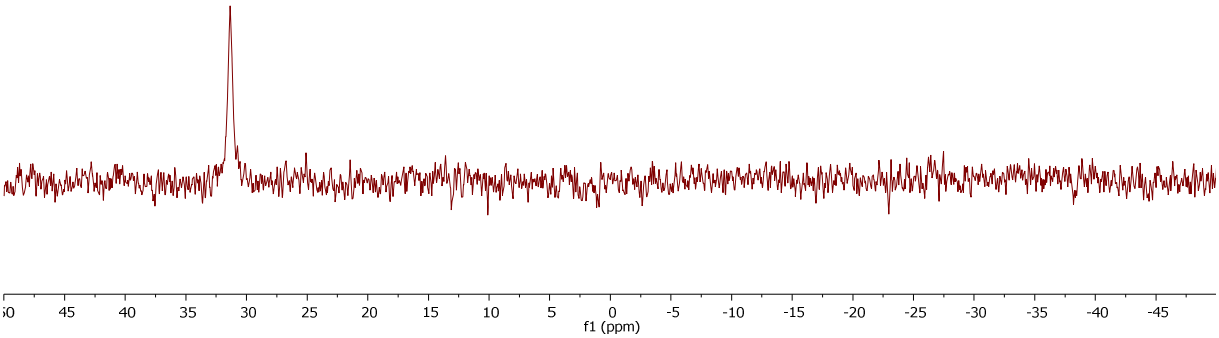

Figure S47. $^{31}P\{^{1}H\}$ NMR (162 MHz, $CDCl_3$) spectrum of **7a**.

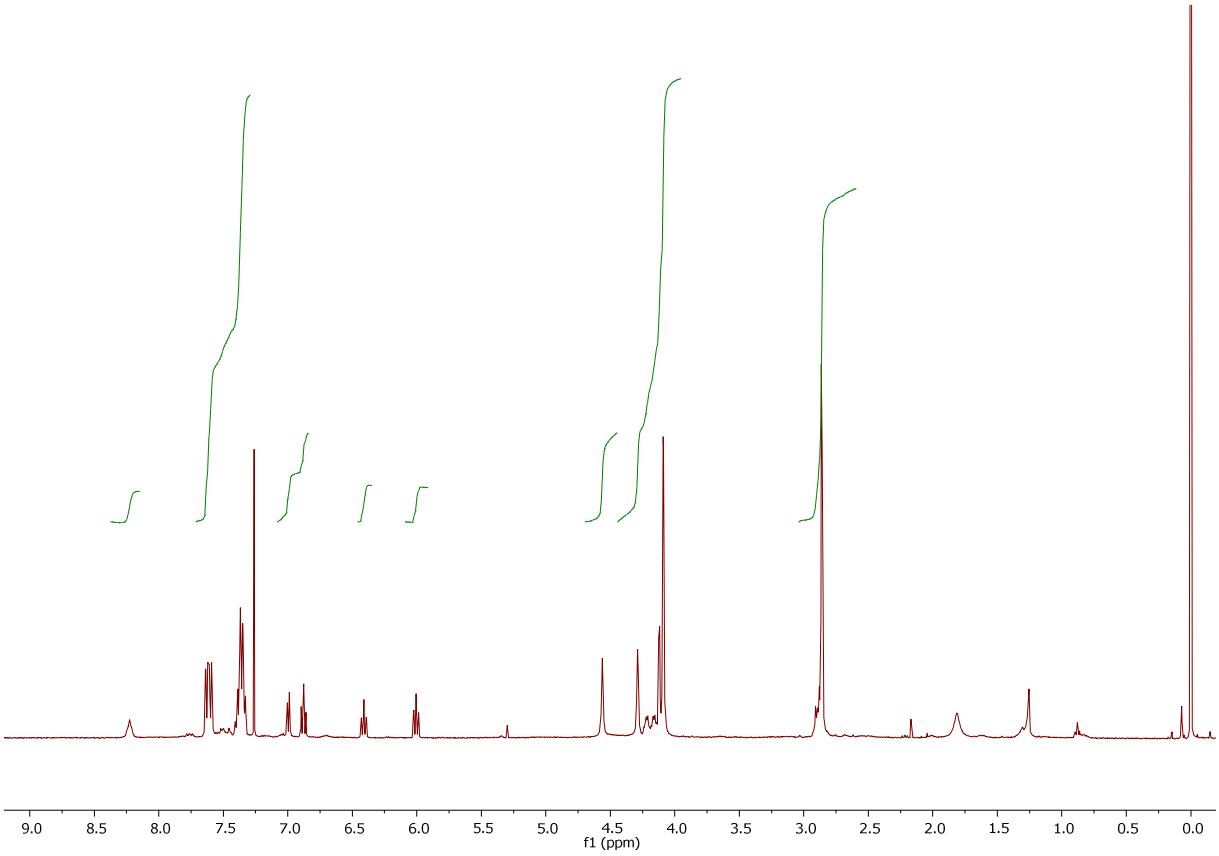

Figure S48. ^{1}H NMR (400 MHz, $CDCl_3$) spectrum of **7b**.

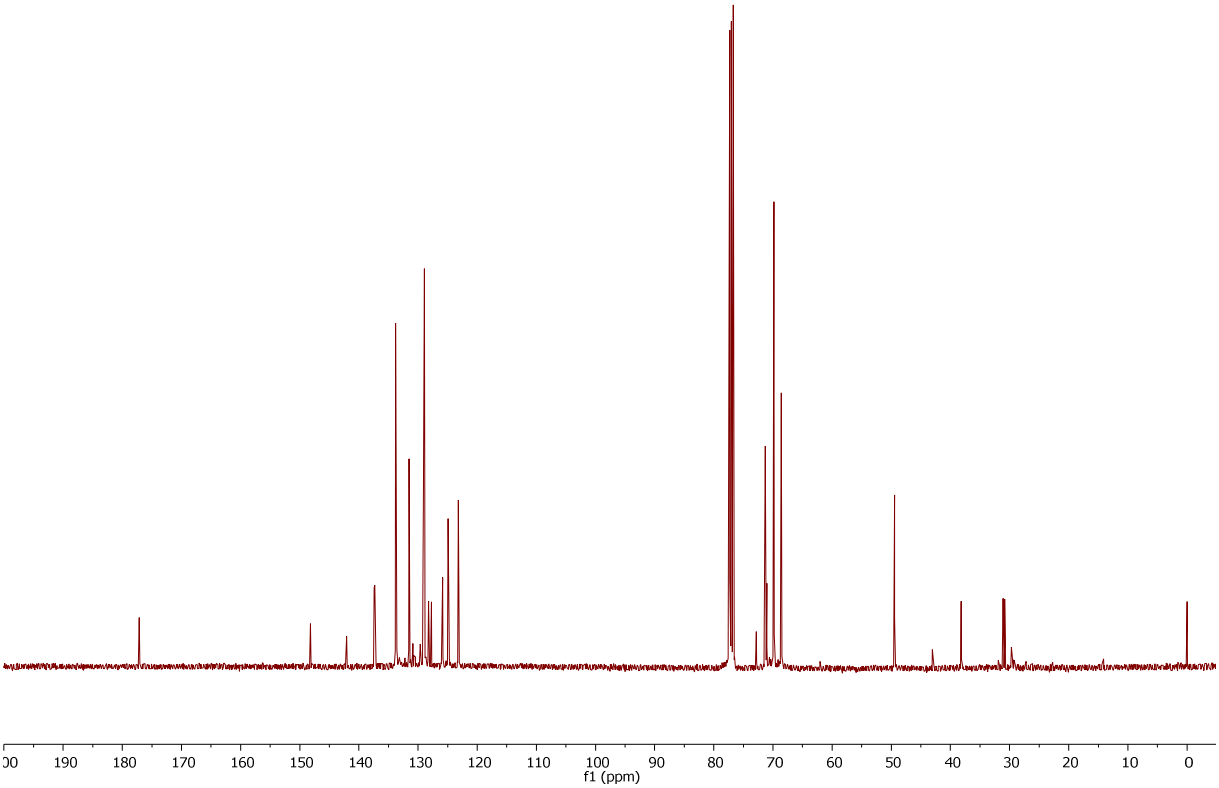

Figure S49. $^{13}C\{^{1}H\}$ NMR (101 MHz, $CDCl_3$) spectrum of **7b**.

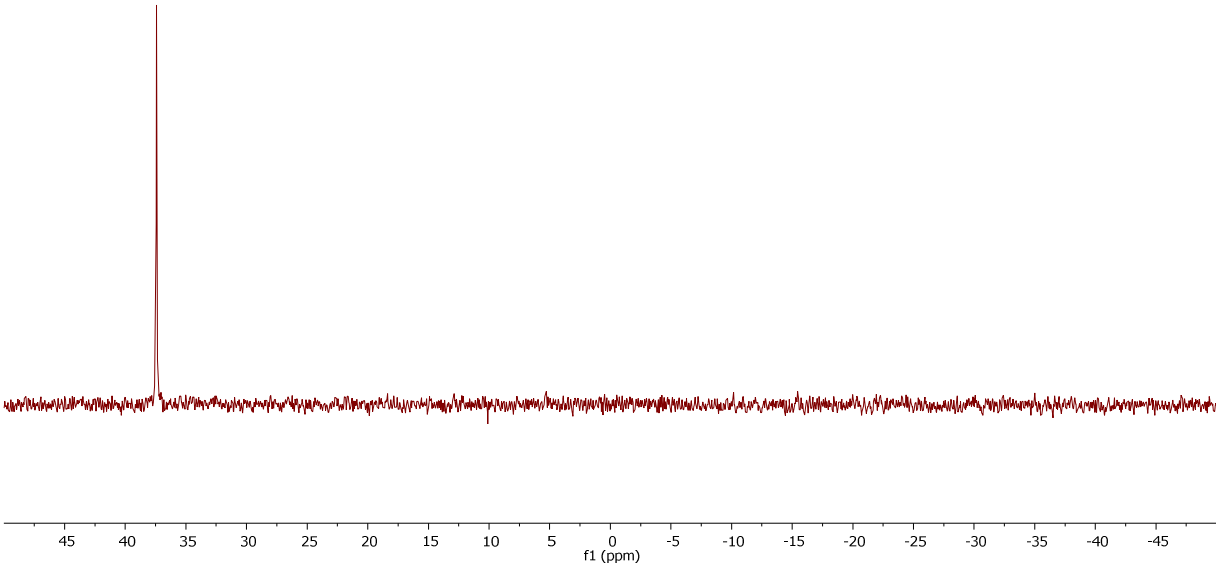

Figure S50. $^{31}P\{^{1}H\}$ NMR (162 MHz, $CDCl_3$) spectrum of **7b**.

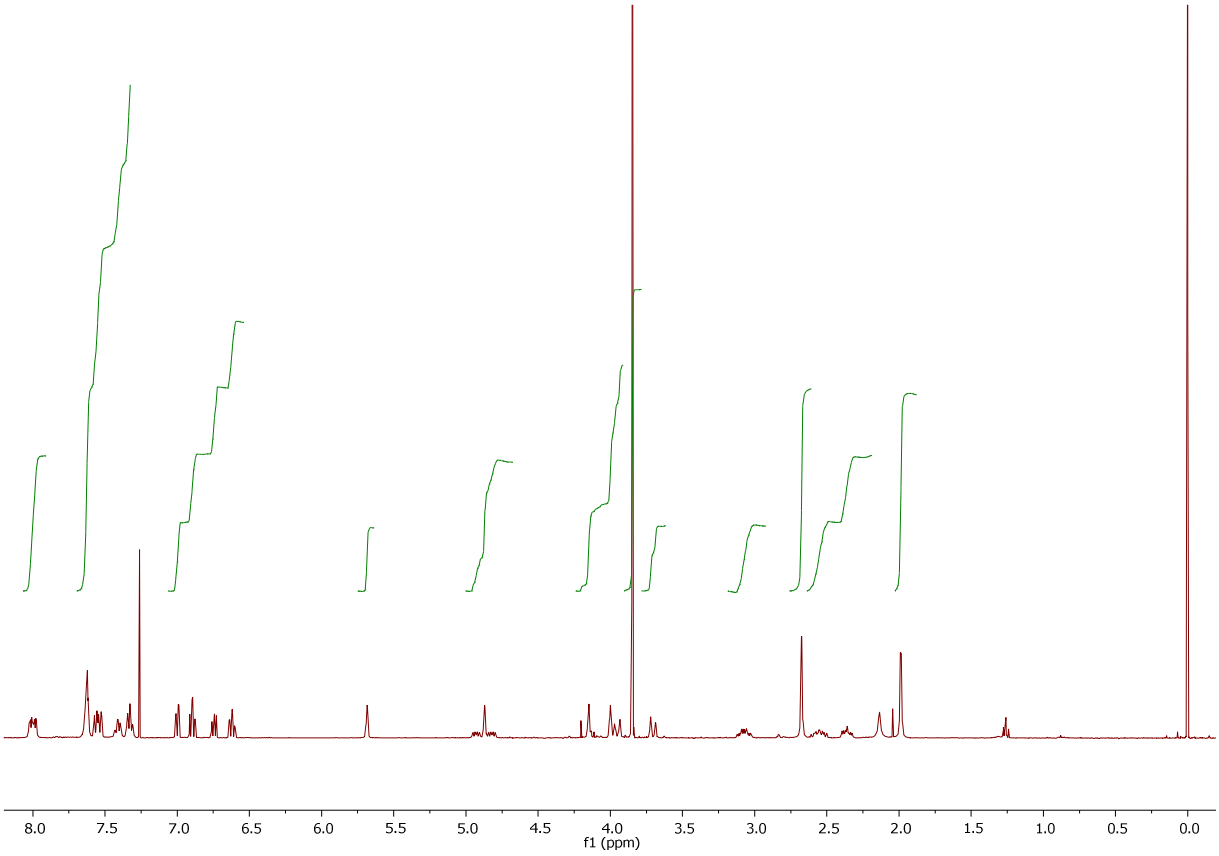

Figure S51. ^{1}H NMR (400 MHz, $CDCl_3$) spectrum of **8**.

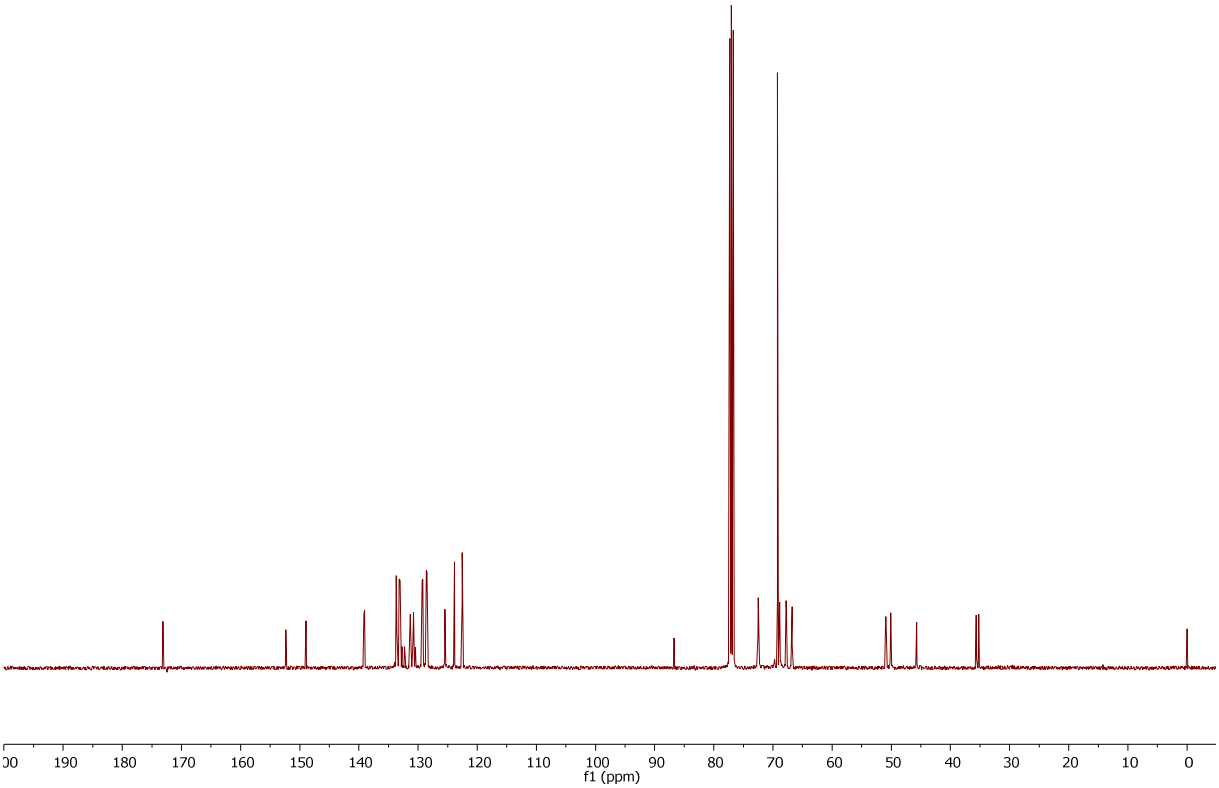

Figure S52. $^{13}C\{^{1}H\}$ NMR (101 MHz, $CDCl_3$) spectrum of **8**.

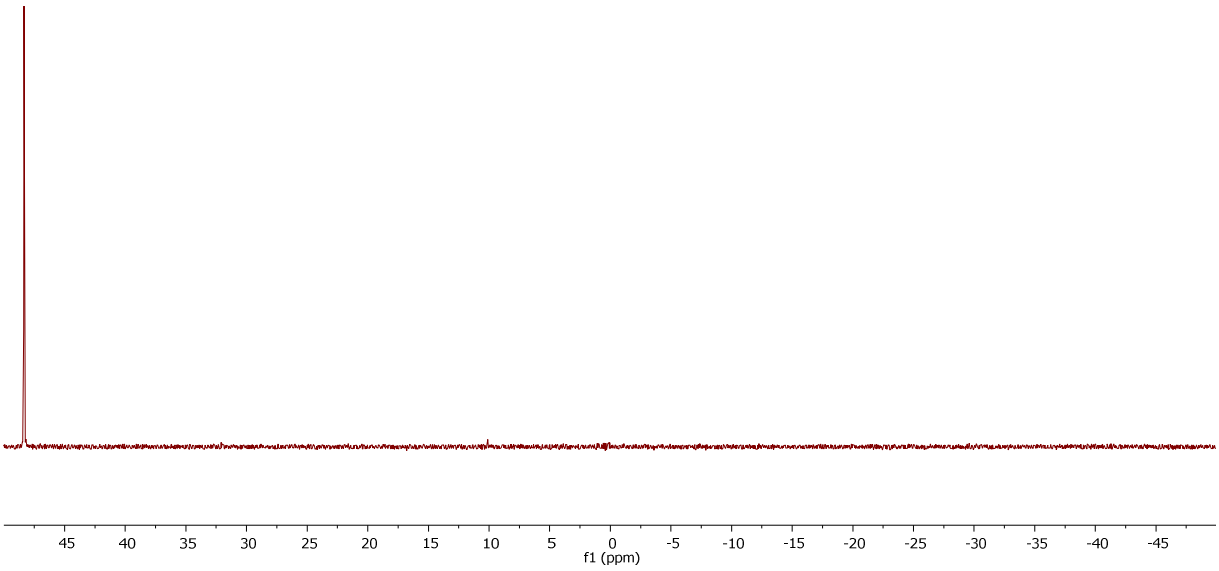

Figure S53. $^{31}P\{^{1}H\}$ NMR (162 MHz, $CDCl_3$) spectrum of **8**.

REFERENCES

S1 H. Goitia, Y. Nieto, M. D. Villacampa, C. Kasper, A. Laguna and M. C. Gimeno, *Organometallics*, 2013, **32**, 6069.

S2 A. R. Katritzky, H.-Y. He and K. Suzuki, *J. Org. Chem.*, 2000, **65**, 8210.

S3 P. Štěpnička, H. Solařová and I. Císařová, *J. Organomet. Chem.,* 2011, **696**, 3727.

S4 P. C. Reeves, *Org. Synth.,* 1977, **56**, 28.

S5 D. Hür, S. F. Ekti and H. Dal, *J. Organomet. Chem.*, 2010, **695**, 1031.

S6 P. Štěpnička, M. Verníček, J. Schulz and I. Císařová. *J. Organomet. Chem.,* 2014, **755**, 41.